UTRECHT UNIVERSITY

Early warning signals of catastrophic regime shifts in semi-arid vegetation-soil systems with slow transients

Author:

George Efstathiou

Supervisor:

Dr. Derek Karssenberg

A thesis submitted in fulfilment of the requirements for the degree of Master of Science

in the
Faculty of Geosciences
Department of Physical Geography

June 17, 2015

Declaration of Authorship

I, George Efstathiou, declare that this thesis titled, 'Early warning signals of catastrophic regime shifts in semi-arid vegetation-soil systems with slow transients' and the work presented in it are my own. I confirm that:

- This work was done wholly or mainly while in candidature for a master's research degree at Utrecht University.
- Where any part of this thesis has previously been submitted for a degree or any other qualification at Utrecht University or any other institution, this has been clearly stated.
- Where I have consulted the published work of others, this is always clearly attributed.
- Where I have quoted from the work of others, the source is always given. With the exception of such quotations, this thesis is entirely my own work.
- I have acknowledged all main sources of help.
- Where the thesis is based on work done by myself jointly with others, I have made clear exactly what was done by others and what I have contributed myself.

Signed: *George Efstathiou*

Date: 17 June 2015

"It is either easy or impossible."

– Salvador Dalí

Abstract

Real world complex systems, such as ecosystems, can undergo abrupt and radical qualitative changes in their states. This comes about when the system crosses a critical threshold, also referred to as a tipping point. Such dramatic shifts between alternative stable states, known as catastrophic regime shifts or critical transitions, are inevitably accompanied by sizeable ecological and economic losses; it therefore gets inestimably valuable to forewarn and avert them. Although prognosticating ecological transitions is a seemingly problematic issue, auspiciously, the detection of a general class of diagnostic indices – the so-called early warning signals, has been recently demonstrated by different methods utilising simple mathematical models. These warning indicators are essentially statistical anomalies starting to be seen ahead of the unwanted collapse, appearing to be applicable to a broad variety of dynamical systems. Recent studies made clear that it can be that many systems might exhibit slow transients between the alternative domains of attraction owing to low rates of change in the system after a tipping point has been crossed. Reviewing the crux of the concept of critical transitions in complex dynamic systems together with the proposed early warning indicators, we centre around a dryland ecosystem that undergoes a catastrophic regime shift from a vegetated to a bare desert ecological state through a fold bifurcation. We systematically explore the rate of change during the transient of the system along with the detectability of the potential early warning signals. The main goal of the study is to acquire more insight into the transient behaviour of semi-arid land surface systems that exhibit long transient periods, evaluating how fast the transition unfolds after transgressing a threshold and what are the early warning signals that may be detected in such systems. We employed a two-dimensional lumped model which describes the dynamics of two coupled environmental compartments – a slow component, the soil subsystem and a fast, the vegetation subsystem – under the effect of grazing pressure. A scenario analysis demonstrates that soil parameters (i.e., bare bedrock weathering rates) significantly influence how quickly the transition unfolds after crossing the tipping point. Importantly, the shift between the contrasting states can be either rapid, unfolding over a period of a few years or unexpectedly slow, responding over centuries or more. Early warning signals in biomass can be observed in the form of increasing variance and declining skewness prior to the critical point, whereas statistical signatures of soil time series seemed to fail detecting the critical change. Further, when the system exhibits a transient phase (unfolding very slowly), early indicators hardly provide a timely warning of the actual shift. Our findings underline the great uncertainty involved when it comes to predict critical transitions explained by the prolonged transient phase together with the system dynamics after transcending the critical point.

Keywords: catastrophic regime shift, critical transition, early warning signals, leading indicators, critical threshold, tipping point, transient dynamics, rate of change, variance, skewness, slow transition, vegetation, soil, semi-arid regions, uncertainty, time series.

Acknowledgements

It is with great pleasure to acknowledge the people that have conduced to the successful completion of this master's research project at Utrecht University.

First of all, I would like to gratefully and sincerely thank my thesis supervisor dr. Derek Karssenberg for giving me the opportunity to work on such an interesting project, and importantly, for his great guidance throughout the course of the project. I am further thankful for his willingness and enthusiasm to promptly answer to all my questions and queries. His role as mentor has been extremely useful and irreplaceable and I believe that I have been exceptionally fortunate to find him as my supervisor.

I must express my gratitude to Maria for her continued support. I thoroughly appreciated her careful proofreading and best suggestions. She helped me in countless ways, but even more, she provided me with encouragement and wisdom.

Last but not least, I would like to express a special feeling of gratitude to my family, my parents Vasilis and Anastasia and my lovely sister Johanna for the unfailing support and love they provided me through my entire life. To them I dedicate this thesis.

Contents

List of Figures

List of Tables

to my family

Chapter 1

Introduction

Naturally enough, gradual changes in the external conditions of ecosystems typically result in gradual, unsurprising and reversible transitions in their states (or 'regimes'). However, sporadically, precipitous radical changes might occur. This means that a system keeps inert until the gradually changing environment passes a certain threshold (i.e., critical point or tipping point or bifurcation point) marking a sudden change from an original to another contrasting state. Such abrupt responses – so-called catastrophic regime shifts or critical transitions – have been described across an array of complex dynamical systems including ecosystems (Scheffer et al., 2009). Catastrophic regime shifts go hand in hand with broad-ranging dire consequences for ecosystems, inasmuch as irreversible changes (i.e., sizeable loss of ecosystem functioning) may be brought about. This, in turn, might strongly affect the human well-being, which relies on ecosystem services.

Critical transitions can likewise be identified in ecohydrological systems, located in dry regions. Climatic variations (e.g. precipitation) or human activities (e.g. grazing) influence such arid ecosystems resulting in sharp shifts from a vegetated state to a bare desert state (Noy-Meir, 1975; Schlesinger et al., 1990; Scheffer et al., 2001; Rietkerk et al., 2004; Foley et al., 2003; Saco et al., 2007; Kéfi, 2008). This is commonly related to the process of desertification which is a serious problem in arid regions.

Arid ecosystems presently occupy about 41% of the Earth's land surface and are home to over 2 billion inhabitants including about a couple of hundred million people in the less-developed world; it is also estimated that 10 to 20% of these drylands are already degraded (Reynolds et al., 2007). The persistent degradation of dryland ecosystems has a detrimental effect on a great many living beings in view of the fact that it carries enormous ecological, economic and social costs. Therefore, we could say that at the present time it constitutes a large environmental challenge (MEA, 2005). In this context,

it would be useful and absolutely vital to make headway towards creating measures that can foretell the probability and the timing of a catastrophic degradation.

Although forecasting critical transitions is a thorny issue (Clark et al., 2001; Kleinen et al., 2003; Guttal and Jayaprakash, 2009; Dakos et al., 2010, 2011; Karssenberg and Bierkens, 2012; Kéfi et al., 2014) several studies put forward that some system variables do change before the regime shift in ways that allow us to discern the proximity of a system to a drastic transition (Scheffer et al., 2009). Such warning signals are indicators of a general phenomenon known in dynamical systems theory as 'critical slowing down' (Wissel, 1984; Strogatz, 1994). This happens in the generality of bifurcation points when the dominant eigenvalue of the system tends to zero. This denotes that when approaching a transition, the return time to equilibrium after a perturbation is getting bigger, signifying that a disturbed system calls for more time to recover when it nears a transition (Van Nes and Scheffer, 2007).

Early warning signals can be direct consequences of critical slowing down (e.g. slow recovery from perturbations, increasing autocorrelation, increasing variance); alternatively they can be linked to asymmetries in the stability landscape or even jump between alternate states (e.g. skewed responses, flickering). Quite possibly, the salient feature of early warning signals hitherto proposed, is that they can be applicable in a wide variety of dynamical systems with multiple attractors. This generic character is founded on the common mathematical properties that are revealed as the system is on the brick of crossing a critical point (or threshold).

Generic early warnings or leading indicators have been recently assessed on ecological time series observations by different methods (e.g. increasing autocorrelation (Ives, 1995; Held and Kleinen, 2004; Dakos et al., 2008; Scheffer et al., 2009), increasing variance (Brock and Carpenter, 2006; Carpenter and Brock, 2006), shifts to low frequency variance (Kleinen et al., 2003; Biggs et al., 2009), changing skewness (Guttal and Jayaprakash, 2008), conditional heteroscedasticity (Seekell et al., 2011)). Moreover, using spatial information for systems allow us to identify additional (and possibly more powerful (Dakos et al., 2010; Scheffer et al., 2012)) predictive measures of imminent transitions (e.g. increasing spatial correlation (Dakos et al., 2010), increasing spatial variance (Oborny et al., 2005; Guttal and Jayaprakash, 2009; Donangelo et al., 2010), peak spatial skewness (Guttal and Jayaprakash, 2009)). The statistical discernment of these early warning indicators is comparatively simple to measure since they do not depend on the complete understanding of the processes of the system (Carpenter and Brock, 2006).

Model studies embodying spatial scales and water-vegetation positive feedback mechanisms (e.g. Rietkerk et al. (2000)) put forward that in a similar vein, the vegetation

patchiness may be used to identify indicators that can foresee and possibly forestall incipient regime shifts (von Hardenberg et al., 2001; Rietkerk et al., 2004; Kéfi et al., 2007). A striking manifestation of drylands is that the vegetation cover consists of a mosaic or pattern made up of discrete patches with high vegetation cover coexisting with sparsely vegetated, or bare ground patches, dispersed across the landscape (Montana, 1992; Aguiar and Sala, 1999; Valentin et al., 1999; Alados et al., 2004; Barbier et al., 2006; Saco et al., 2007); seeing that in such water-limited ecosystems there is an adaptive advantage to plants of making localised aggregations rather than organising homogeneously (Sherratt, 2013). The vegetation pattern formation differs in scale and shape and it depends on slope and rainfall (von Hardenberg et al., 2001; Rietkerk et al., 2002).

For the most part, catastrophic regime shifts are considered to be sharp and short-lasting. Nonetheless, on a more subtle level, for many systems it is not known how quickly the transition unwinds, once a critical threshold is passed. This is to say that they may often exhibit slow transient responses and thus, this can be a serious impediment to the prevention or reversion of imminent ecological transitions (Hughes et al., 2013). Importantly, the rate of change (fast or slow) throughout the course of the transition turns on the response time of the system (Hughes et al., 2013). In a slowly unfolding regime shift, occasionally, the transient can be first slow and then fast, especially in a mixed system consisting of a slow and a quick component (e.g. Karssenberg (2014)).

In this study, we focus on the occurrence of a critical transition in a hillslope system within a semi-arid ecosystem triggered by overgrazing or climate change. To be more specific, the system switches from a healthy state, with high vegetation cover and well developed soils, to a degraded state with low or no vegetation cover and largely degraded soils.

Seeking properties of the system that may noticeably change as the regime shift to a barren state is neared, we check whether statistical properties of the state variables in the system provide ample advance warning to avoid the adventitious degradation. We ponder how fast the critical transition unfolds and we look at the potential early warning signals.

This is done in a modelling study. We consider a distributed hillslope evolution model (Karssenberg, 2011) that simulates the transition from a vegetated hillslope with thick soils (i.e., healthy state) to an unvegetated, bare-soil hillslope (i.e., degraded state), having as main output a time series of hillslope geometries (i.e., topographical surface, development of gullies, regolith thickness) and vegetation coverage. Principally, we utilise a spatially-lumped model (Karssenberg, 2014), which is defined from the spatially-distributed model and solely represents the fundamental processes of the vegetation-soil

system. The lumped model is composed of two coupled differential equations describing the interaction between the vegetation and the soil system. The system is mainly driven by the grazing rate (increasing grazing intensity engenders a decrease in vegetation cover and soil thickness). To this effect, the main objectives of our research strive to address the following questions:

- How fast does the land surface system collapse when the grazing threshold is exceeded?
- What early warning signals emerge in advance of the catastrophic regime shift in the vegetation-soil system and in which components of the model do these early warnings occur?
- Considering a transient behaviour by the system, can we observe discernible changes in the statistical values subsequent to the actual shift point that may be useful as early warning signals and how do they rest on the key parameters of the soil system such as bedrock-weathering rate?

We implement an innovative approach working in a recently-emerged large body of literature on catastrophic regime shifts and early warning signals. We systematically examine the system's behaviour, while modifying the soil parameter values, with main focus the weighing of the lumped model for early warning indicators by statistically analysing its outcome.

The overall structure of this thesis takes the form of six chapters, including this introductory chapter 1. The remainder of this work is organised in the following way: In chapter 2, we provide a brief description of the theoretical background for the phenomenon of critical transitions outlining essential concepts of dynamical systems theory. We also give a thumbnail sketch of the several early warning signals as predicted from the theory. We centre upon critical transitions in arid ecosystems, a well known exemplar of tenuous ecosystems prone to lose their vegetated state and dramatically switch to a desertified state owing to external perturbations or system's internal dynamics. Within this chapter, we further provide a broad overview of the ecohydrological and geomorphological characteristics of such water-limited systems. Chapter 3 is devoted to the methods utilised in this research project giving an account of the models employed to evaluate the prospective early warning signals along with the way of analysing the simulation results from these models. It is followed by chapter 4, wherein the results of our simulations are presented. Next, we discuss our findings together with future research directions in chapter 5. Finally, we draw our conclusions in chapter 6.

Chapter 2

Background Theory

In this chapter, we present a literature review on the rudiments of the theory of critical transitions, paying particular attention to catastrophic regime shifts in semi-arid ecosystems. We shed light on the pieces of theory of generic early warning signals, such as the notion of critical slowing down, giving various examples of these indicators.

2.1 The basics

Dynamical systems theory is a field of mathematics utilised to describe the behaviour of complex dynamical systems. A dynamical system can be any system (e.g. ecosystems, financial markets, physiological systems and the climate), which is retained in a dynamic equilibrium by forces acting against each other. To paraphrase, it is anything that its state can be grasped as a balance of processes (Scheffer, 2009). For instance, the number of species on an island represents a balance between the rate of immigration to the island by new species and the rate of extinction of species on the island (MacArthur and Wilson, 1963, 1967) (figure 2.1).

Interestingly, ecosystems are in fact never in equilibrium meaning that they do change over time – there are always slow trends or continuous fluctuations of species populations (Scheffer and Carpenter, 2003). Nonetheless, even if the environmental conditions remained the same, population dynamics would fluctuate. For example, this was put forward by Benincà et al. (2008) who presented the first experimental demonstration of chaos in a long-term experiment with a complex food web isolated from the Baltic Sea. They showed that species interactions in food webs can generate intrinsic deterministic chaos (i.e., system does not have an equilibrium). In this respect, we could say that this is a particular equilibrium of nature (i.e., behaves in unpredictable way) occurring, inter alia, in ecosystems.

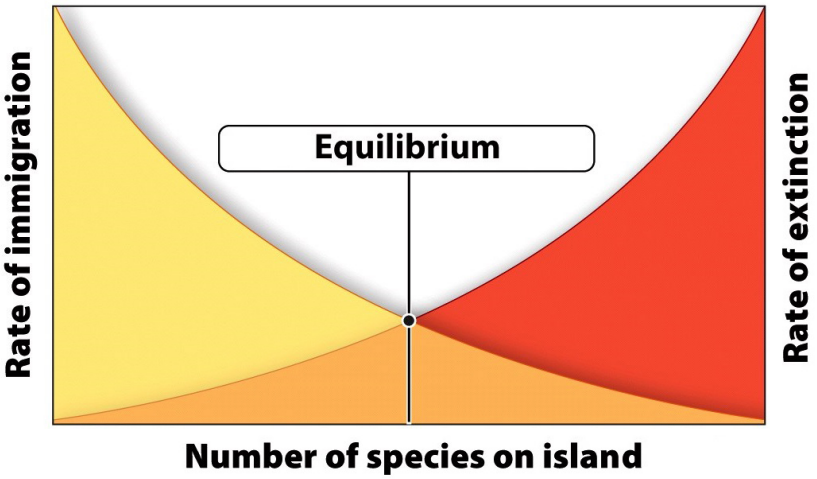

FIGURE 2.1: The concept of the equilibrium theory illustrated for island species densities. At equilibrium, immigration balances extinction and different species exist on the island. This means that the number of species on the island remains roughly the same. Nevertheless, while the number of species does not change, the composition of those species on the island may change (modified from Phelan et al. (2009)).

In parenthesis, to keep away from misreading, it is important to note here the difference between chaos and stochasticity. Chaotic systems go along with deterministic rules having high predictability for a short period of time, contrastingly stochastic fluctuations occur to a certain degree by chance – so stochastic systems are solely predictable in terms of probabilities (Benincà, 2010).

Sometimes, nonetheless, precipitous and unexpected shifts are observed, e.g. major regime shifts in oceans, lakes, rangelands (Scheffer et al., 2001). These changes are often caused by a major external impact, but more interestingly, the system might growingly become brittle up to the point that a slight perturbation can trigger a radical change.

In this regard, we could symbolically liken a complex system to a ship that is being designed dangerously by increasing its size to pile more passengers aboard. Just as such a ship is inherently unstable and a minor wave can tip its balance, a complex system can slowly lose resilience until even a tiny perturbation can trigger a large shift in the system by passing a critical point.

Comprehending when complex systems become brittle may be quite puzzling, nevertheless the fact that they might be governed by some common identifiable underlying principles such as dynamic equilibrium or tipping points suggests that under certain conditions many systems can behave in such drastic and unforeseeable way.

2.2 Types of transitions

Abrupt transitions occur when the gradually changing environment passes a critical point or when discrete perturbations bring about sudden shifts in the underlying environmental drivers (Scheffer et al., 2001). Such abrupt responses triggered by small forces, symbolise the so-called catastrophic bifurcations (Scheffer and Carpenter, 2003). The term 'catastrophic' is understood to refer to the mathematical field of catastrophe theory which is a branch of bifurcation theory in the study of dynamical systems and has its origin in the work of the French mathematician René Thom in the 1960s (Thom, 1974). It classifies phenomena in systems characterised by drastic shifts arising from small changes in circumstances (Kéfi, 2008).

There is a plethora of paradigms of ecosystems exhibiting such dramatic regime shifts, including marine and coastal environments (e.g. Glynn (1988); Done (1992); Knowlton (1992); Hughes (1994); Estes and Duggins (1995); Steele (1996); McCook (1999); Petraitis and Dudgeon (1999); Worm et al. (1999); Hare and Mantua (2000); Nyström et al. (2000); de Roos and Persson (2002); Steneck et al. (2002); Daskalov et al. (2007)), fresh water systems (e.g. Blindow et al. (1993); Scheffer et al. (1993); Scheffer et al. (1997); Carpenter et al. (1999); Gunderson (2001); Walters and Kitchell (2001); Post et al. (2002); Carpenter (2003); Jackson (2003); Scheffer et al. (2003); Scheffer (2004); Carpenter (2005); Scheffer and Jeppesen (2007)), and terrestrial ecosystems (e.g. Dublin et al. (1990); Walker (1993); Bisigato and Bertiller (1997); Brown et al. (1997); Anderies et al. (2002); D'Odorico and Porporato (2004); Peters et al. (2004); Rietkerk et al. (2004); Bestelmeyer (2006); Schmitz et al. (2006); Narisma et al. (2007)).

Such catastrophic regime shifts ensue from systems with alternative stable states (or alternative attractors), referring to a system of having more than one stable state under the same external conditions. Typically, alternative stable states rest upon the presence of positive feedback mechanisms. Positive feedbacks usually involve biological and physical processes (Rietkerk and Van de Koppel, 1997; Scheffer et al., 2001), examples thereof including, inter alia, trophic cascades (Carpenter et al., 1999), land surface climate feedback (Foley et al., 2003), spreading desertification (Peters et al., 2004).

An intuitive denotation for comprehending the implications of alternative stable states is stability landscapes, shown in figure 2.2d. The position of the ball in the landscape corresponds to the state of the system, and the bottom of the valleys illustrates the alternative states. The range of conditions that lead to equilibrium set the basins of attraction (or domains of attraction) of the two alternative states of the system. The ball rolls down the hillsides and is at rest at the lowest part of the valleys representing equilibrium.

There are two manners in which a system can move from one stable state to another. The first way is by a quite large perturbation which is applied directly to the state variables (shift in variables), and the second one is by a change of the landscape per se owing to changes in external conditions (shift in parameters) (Beisner et al., 2003). The size of the basin of attraction plays a crucial role in how easily the system might be displayed from its equilibrium; the larger the basin of attraction is, the more likely the system is to return to its initial state.

In terms of Holling (1973), the magnitude of perturbation a system can stand before it shifts to a contrasting state is referred to as the resilience of the system. As the system reaches the critical threshold, the size of the attraction basin becomes small, resilience is small as well, and even a minute perturbation might bring the system into the contrasting basin of attraction.

Figure 2.2 shows the different types of transitions, together with how external conditions can affect the resilience of equilibria. A transition in a system can be induced by an external forcing (e.g. climate, human pressure). Some systems' state may react in a smooth continuous way to such perturbations. For instance, if a system behaves almost linearly, a change in system state may be caused by a large external force (figure 2.2a).

In other instances, small changes in conditions can result in disproportionally large changes in the state of the system – although a reversal of conditions of an equally small magnitude can reverse the regime shift (figure 2.2b).

Alternatively, however, it can be that tiny changes in conditions may hasten extreme discontinuous responses that are most likely irreversible (figure 2.2c). This occurs when at a threshold, the system precipitously shifts towards a different state. In the first and the second situation (figure 2.2a,b), there is only one stable state, but in this third response (figure 2.2c) reinforcing feedbacks determine two alternative states.

On very many occasions, it has been erroneously proposed that these three aforementioned equilibria responses are said to be gradual, sudden and catastrophic – but actually, the rate of response by the systems to a change in conditions or driver variables may vary from quick to slow, depending on the response time of the system in every case (Hughes et al., 2013). Thus, in line with Hughes et al. (2013), in order to avoid misinterpretation, we consider that the response (at equilibrium) can be smooth and reversible (figure 2.2a), threshold and reversible (figure 2.2b) and hysteretic (alternative attractor) (figure 2.2c).

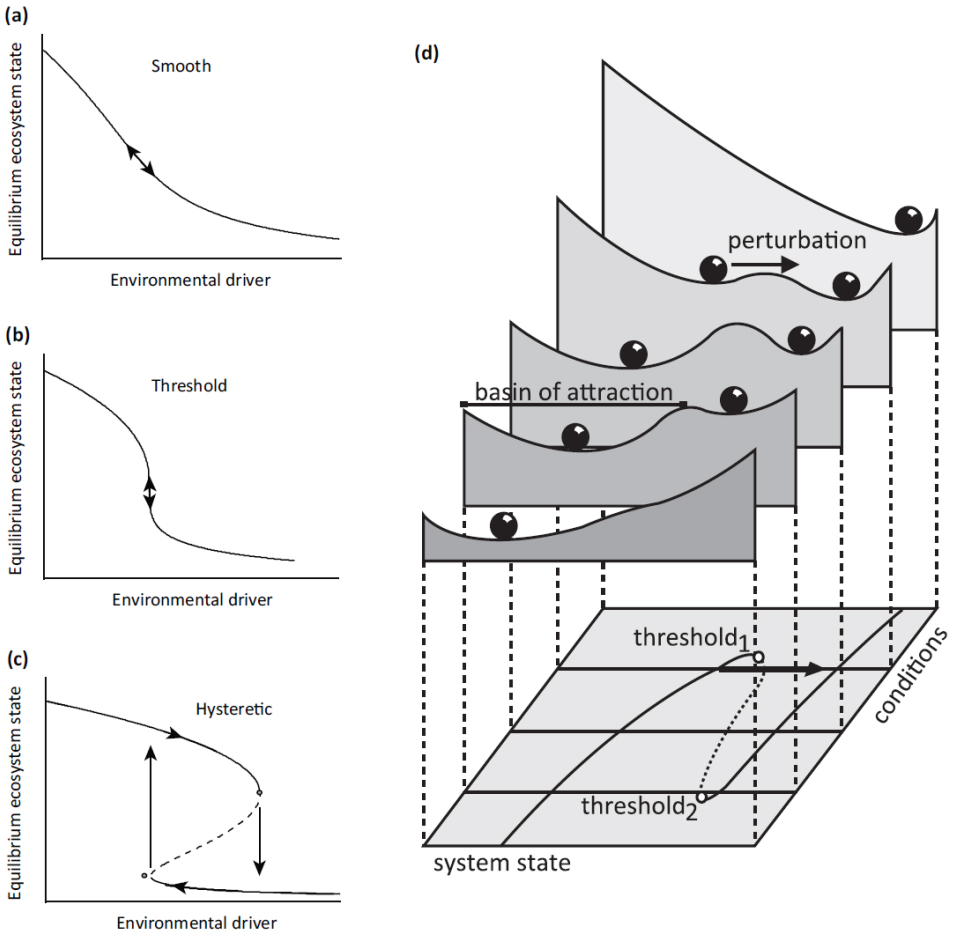

FIGURE 2.2: Depiction of the different responses of a dynamic system to change in conditions: (a) Smooth and reversible response: changes in the state of the system foreseeably occur. (b) Threshold and reversible: the state of the system reacts in continuous expected way. (c) Bi-stability and hysteresis: adventitious change of the system (transition between two alternative states) (taken from Hughes et al. (2013)). (d) Stability landscapes exemplifying the transition of a system state between two alternative stable states. The ball in the landscape represents the state of the system and the valleys represent the basins of attraction that correspond in stable equilibria. The motion of the ball denotes the change in the state of the system and the slope of the landscape corresponds to the rate of change. The bottom plane shows the equilibrium curve. The ball rolls down the hill and becomes firm representing equilibrium situations. As getting close to the critical threshold 1, the basin of attraction contracts (i.e., the system becomes less stable) up to the point that a minute perturbation may tip it out of the basin of attraction to the alternative state. White points threshold 1 and threshold 2 indicate catastrophic bifurcations (taken from Dakos (2011)).

Although it is generally believed that regime shifts between alternative states are depicted as sharp and radical, it can often be that transitions unfold for a length of time and may also require more time to reverse (Hughes et al., 2013). Systems behaving as such, undergo a gradual transient response following the passing of a tipping point, and this can be due to the low rate of change in the system (Karssenberg, 2014). Figure 2.3 shows a paradigm of how fast- and slow-responding systems change throughout the transition, depicting the modelling response of an ecosystem to a driver of change.

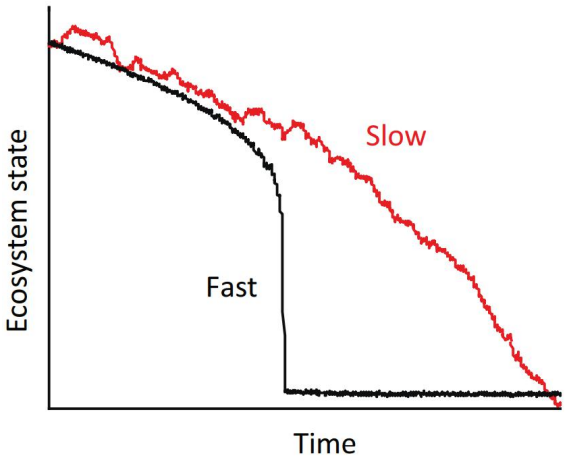

FIGURE 2.3: The modelled response of how fast (black)- and slow (red)-responding systems change through time after a threshold has been reached (taken from Hughes et al. (2013)).

Interestingly, it can be observed that the system responding at a slow pace is most of the time in transient state when crossing a critical threshold. Thus, a major issue that emerges from this specifically relates to the capacity to prognosticate and anticipate such regime shifts.

2.3 Early warning signals for critical transitions: a review

2.3.1 Critical slowing down and its manifestations

As complex systems (e.g. ecosystems) are on the brink of crossing a tipping point, their dynamics are related to a phenomenon known in dynamical systems theory as 'critical slowing down' (Wissel, 1984). A straightforward manner to comprehend why we should anticipate early warnings before critical transitions is by thinking of the fate of a globe in a landscape of hills and valleys (figure 2.4). Balls represent the state of the system and valleys correspond to the basins of attraction. The size (i.e., width and steepness) of the basin of attraction is a measure of the maximum disturbance that a system can absorb without shifting to an alternative state and it reflects the resilience of the state of the system (Holling, 1996) (figure 2.4a,b).

As the system comes near to a critical transition, the basin of attraction of the current state of the system gets smaller and so does its resilience. Even a minute perturbation may shift the sphere to another valley. The steepness of the basin of attraction simultaneously lowers meaning that, although the same perturbation that may not tip the system, it will definitely take longer to dissipate, leading to the phenomenon of critical slowing down (figure 2.4c,d).

In technical terms, when approaching a fold bifurcation point the dominant eigenvalue that characterises the rate of change around the equilibrium tends to zero. Critical

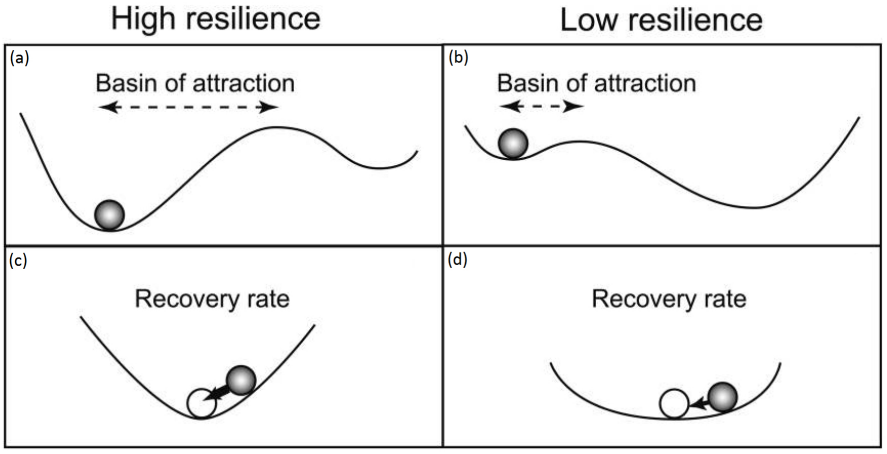

FIGURE 2.4: Stability properties of an ecosystem exhibiting alternative stable states: valleys represent stability domains and balls represent the system. If the size of the attraction basin is large (i.e., stable system), the system will quickly return to its equilibrium when it is slightly perturbed. If the size of the attraction basin is small, resilience is small and even a slight perturbation may bring the system into the alternative basin of attraction (taken from Van Nes and Scheffer (2007)).

slowing down relates to the ability of a system to recover from small perturbations in order to return to its previous state. A system that is able to quickly recover from small perturbations is said to be a stable system. The critical slowing down is the reduction in the speed in which these small changes are recovered from; it can therefore be seen as a slow transition into a less stable state. The reduction in the system's ability to recover leads to a decline in the rate of change within the system, from one time step to the next.

Among others, Scheffer et al. (2009) showed that the slowing down begins to occur far from the bifurcation point (i.e., a critical threshold in conditions at which the qualitative behaviour of a system changes), with the recovery rate reducing smoothly towards this point. The detection of this slowing down can therefore act as an early warning of a catastrophic event (Wissel, 1984; Gandhi et al., 1998; Van Nes and Scheffer, 2007).

A way to detect the slowing down of a system is through measuring its variance. As the system recovery speed reduces, the effects of small perturbations are not removed. The accumulation of these perturbations through time increases the variance. A peak in variance is therefore an indication of an imminent bifurcation (Carpenter and Brock, 2006). Another, quite straightforward way to measure slowing down is to look at autocorrelation. Critical slowing down results in a rise in autocorrelation in advance of the upcoming shift of the system (Held and Kleinen, 2004; Dakos et al., 2008).

2.3.2 Skewness and flickering

In addition to the early warning signals given by a critical slowing down, a system approaching a catastrophic event can be seen to experience an increase in the asymmetry of the fluctuations. At a critical threshold the system slows, resulting in the system state remaining near that critical threshold for longer. This means that the slight fluctuations in the system are skewed towards the threshold value. This skewness can be either higher or lower than the modal value, namely positive and negative skewness. This slowing down occurs until the rate of change in the system immediately prior to the bifurcation is (almost) zero. Thus, we may observe a changing trend (i.e., increase or decrease) of the distribution of skewness in the time series of a state variable close to a tipping point (Guttal and Jayaprakash, 2008).

Another phenomenon that can be observed in the vicinity of a tipping point is termed flickering or stuttering. In highly stochastic environments, large disturbances (i.e., noise) can potentially cause the system to 'flicker' between the basins of attraction of the system's alternative states (Dakos et al., 2013). In such conditions critical slowing down cannot be observed and the efficacy of its related generic indicators in presaging the imminent transition is restricted (Scheffer et al., 2009; Perretti and Munch, 2012; Dakos et al., 2013). Nevertheless, flickering can be detected as a warning signal of alternative stable states and it causes an increase in variance and skewness, as well in bimodality (e.g. Carpenter and Brock, 2006; Carpenter et al., 2008; Wang et al., 2012).

2.3.3 Spatial patterns

In addition to subtle predictive measures in time series, in a more general setting, spatial structure of ecosystems gives us information about the ecosystem degradation level (Kéfi et al., 2014). Critical transitions may be signalled by changes in spatial characteristics of the system. Possibly, spatial patterns may be considered to be more forceful indicators to anticipate regime shifts insofar as containing more information than a single data point in a time series (Dakos et al., 2010).

Several early warning indicators have been proposed for spatial ecological data. In such cases, it has been shown that spatial correlation may increase prior to a transition (Dakos et al., 2010), and by computing the discrete Fourier transform (DFT) spatial spectral properties may change as the system approaches a tipping point (Carpenter and Brock, 2010). In parallel lines, an increase in spatial variance (Oborny et al., 2005; Guttal and Jayaprakash, 2009; Donangelo et al., 2010) accompanied by a peak in skewness (Guttal and Jayaprakash, 2009) could provide early warnings of approaching transitions.

Moreover, it has been suggested that utilising the characteristics of spatial vegetation patterns such as patch-size distributions (Kéfi et al., 2007) or spatial regularity (Rietkerk et al., 2004; Kéfi et al., 2010) acts as early signs of an upcoming transition.

2.3.4 Early warning signals in systems with slow transients

As mentioned earlier, critical transitions between alternative states can unfold either rapidly or slowly (Hughes et al., 2013). For instance, in a slowly unfolding regime shift the transient can be initially slow and then fast, especially in a dynamic system consisting of slow and quick components (e.g. Karssenberg (2014)). Hence, besides the warning signals that can be discerned toward the critical shift point, another forewarning might be picked up above the tipping point.

To the author's knowledge, studies of early warning signals in systems with long-lasting transients do not exist so-far and the detection of diagnostic indices may therefore be formidably challenging. It remains unclear how robust and informative the different early warning signals would be. This give emphasis on the uncertainty related to prognosticating critical transitions in ecosystems (Karssenberg and Bierkens, 2014).

2.4 Ecohydrology and geomorphology of arid ecosystems

2.4.1 Eco-hydro-geomorphic processes

In drylands, impacts of feedback between vegetation, hydrology, and geomorphology are quite tight appearing across different scales (Saco and Rodriguez, 2013), leading to the emergence of banded landscapes consisting of alternating bands of vegetation and bare soil oriented along the topographic contour in some gently sloping. Such patterns ensue from the co-evolution of landforms and biotic components, which makes the understanding of mechanisms causing ecosystem state change, as well as its forecast, greatly challenging (Saco and Moreno-de las Heras, 2013).

Figure 2.5, reproduced from Ludwig et al. (2005), depicts a schematic diagram of hydrological and ecological events and processes appearing on a gentle hillslope. The principal limiting factor in drylands, precipitation (P), falls to the landscape surface (vegetation patches and interpatches) on hillslopes. Infiltration of water (I) moves into deeper layers depending on hydraulic conductivity (K) and soil water might be lost by deep drainage (DD). When the rate of rainfall on the surface exceeds the rate at which water can infiltrate the ground, runoff (RO) occurs that can be captured as runon (RN)

by vegetated patches and stored in soil horizons (ΔS) furthering biological activity (e.g. ants and earthworms) (B), thereby improving infiltrability. Interpatches might have low infiltration rates owing to their vulnerability to soil surface sealing. In contrast, vegetation patches promote greater infiltration in the soil. Soil water is evaporated (E) in bare soil patches and evapo-transpired (ET) within the bounds of vegetated patches. Overland flow might move downslope toward a surface water body (e.g. creek or river) (D).

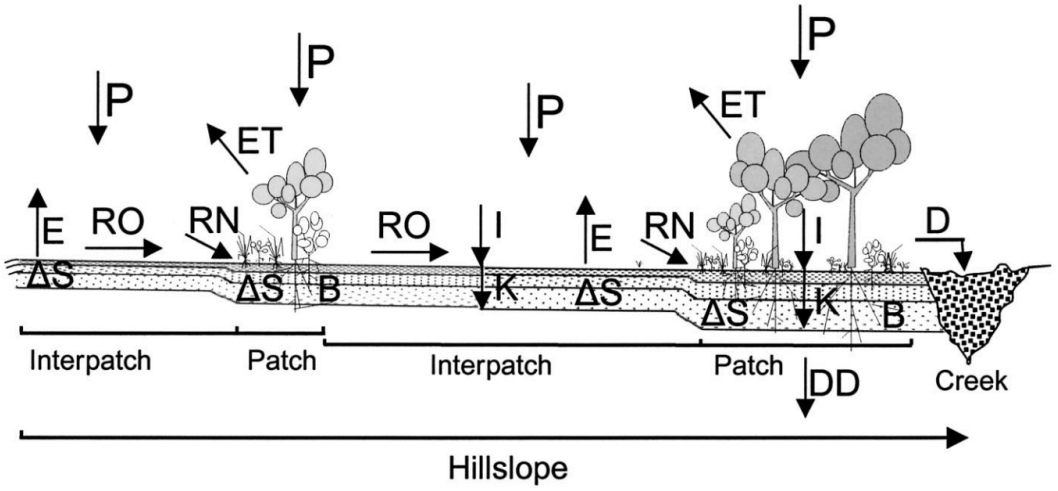

FIGURE 2.5: Schematic diagram illustrating links and interactions between hydrological and ecological events and processes occurring on a hillside. Higher infiltration rates under vegetation set off the generation of runon-runoff mechanism. In this way, this mechanism brings about a positive feedback by giving a rise to soil moisture availability for plant growth (for explanation of symbols, see main text) (taken from Ludwig et al. (2005)).

On the basis of the aforementioned processes, the runoff-runon mechanism can trigger a positive feedback by increasing soil moisture and vegetation growth (Valentin et al., 1999; Wilcox et al., 2003; Saco et al., 2007; Pelletier et al., 2012). Within vegetated patches, higher infiltration leads to higher soil moisture availability, thereby reinforcing the pattern. This redistribution of water from interpatch (source) to patch (sink) regions constitutes a key process in arid landscapes (Saco et al., 2007). Additionally, the redistribution of water by surface flow includes sediment and nutrients.

In their major study, Tongway and Ludwig (2001) reviewed some of the theories about the intriguing question of why banded landscapes form, contending that there are many conjectural viewpoints for their origin. Some put forward that banding is recent and formed from a uniform vegetation cover owing to land use effects by human domination. As another opinion, it may be driven by the climatic shifts over the Holocene, or geomorphic processes (i.e., interactions between the Earth's surface and the natural forces). Furthermore, it might be viewed as the response of vegetation to environmental driving forces (e.g. water and wind), with water playing a predominant role in band formation (Tongway and Ludwig, 2001).

Vegetation bands can be generated in a broad range of drylands all over the world (e.g. in Africa (Thiery et al., 1995), Australia (Ludwig et al., 1999; Dunkerley and Brown, 2002), North America (Montana, 1992; McDonald et al., 2009), Southern Europe (Bergkamp et al., 1999), Western Asia (White, 1969)). Importantly, a fundamental condition in the development of banded patterns is the ability of landscape surface conditions to produce overland flow (Valentin et al., 1999; Tongway and Ludwig, 2001; Saco et al., 2007). This means that in landscapes wherein their surface form prevents the generation of overland flow, no vegetation banding occurs.

2.4.2 Transitions in dry regions

The general mechanism underlying catastrophic regime shifts in water-limited environments is vegetation-climate feedback loops (i.e., feedbacks among precipitation, soil moisture and vegetation) (figure 2.6a). Dryland ecosystems are characterised by the limited water availability and evidently, plant growth is mainly limited as well. Therefore, vegetation cover increases when water availability increases. Similarly and in a converse manner, if vegetation biomass declines (e.g. by increasing aridity or high intensity grazing), less water is available for the vegetation and the remaining water runs off. Further, in the case of severe rain events soil erosion may be caused. In this way, such disturbances may change the structure of vegetation patches. So, there is a range that two alternative stable states can coexist due to the fact that each stable state is stabilised by positive feedback loops (figure 2.6; (Kéfi, 2008)). This case is referred to as the bistability area (Noy-Meir, 1975) and its emergence has provided a great impetus for cognisance of arid ecosystems over the recent decades (Caylor et al., 2014).

Positive feedbacks can lead to a typical spatial pattern distribution of vegetation (Rietkerk et al., 2004). Dryland vegetation is patchy meaning that less-vegetated or bare patches coexist with vegetation patches, ranging in size and shapes. This occurs due to the resource-concentration and local facilitation mechanisms (King et al., 2012; Mayor et al., 2013). In terms of von Hardenberg et al. (2010), there are two fundamental broad categories of spatial vegetation patterns: a) periodic vegetation patterns that have characteristic length scales (e.g. bands on hill slopes or spotted patterns) (Valentin et al., 1999) and b) scale-free patterns that vary in length scales and coexist in the system (Kéfi et al., 2007).

2.4.3 Reviewing previous hydrological and landscape evolution models

Over the past few decades, a plethora of modelling methods have been developed and utilised to simulate hydrological processes in arid areas, including metric, conceptual and

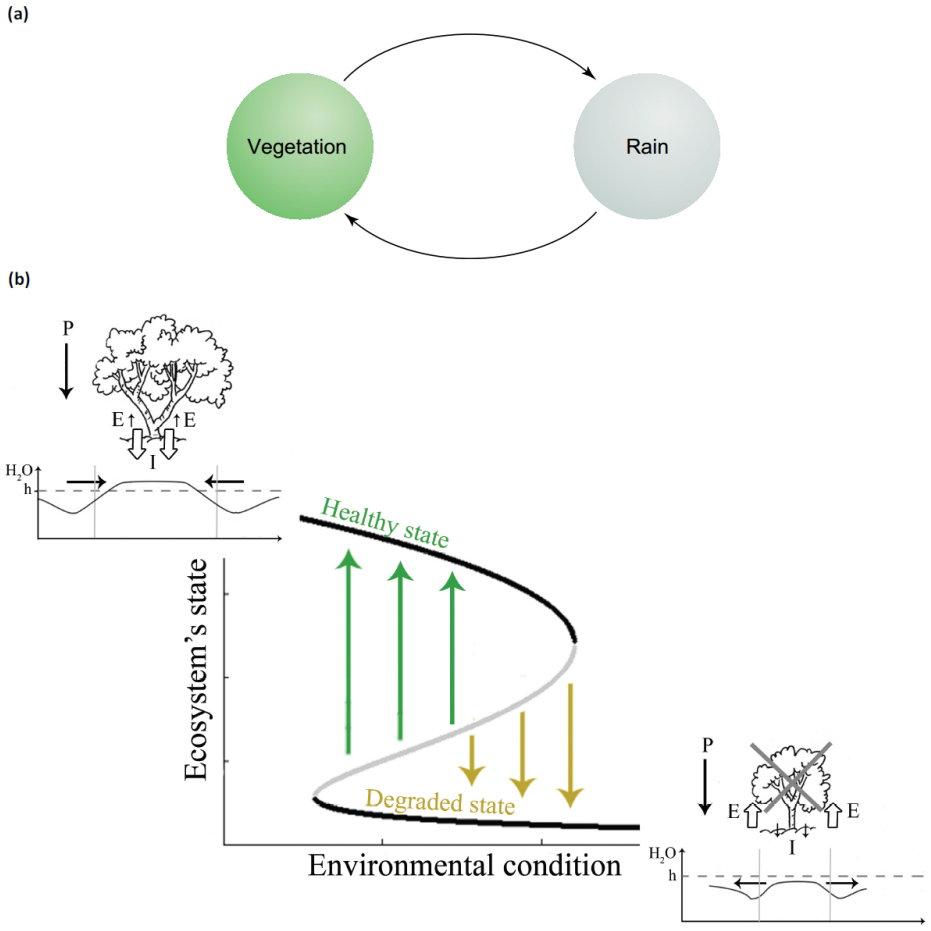

FIGURE 2.6: (a) Vegetation-climate feedbacks in drylands, a positive feedback can arise between vegetation cover and local precipitation (taken from Scheffer and Carpenter (2003). (b) At the centre is the bifurcation graph for May's model (May, 1977). Positive feedbacks are responsible for the existence of two alternative states – one with vegetation (healthy state) and one without (degraded state) – separated by an unstable state (grey line). The arrows show the direction of change if the system is not in one of the stable states. If the initial vegetation is high, it will lead to more water (i.e., high infiltration (I), low evaporation (E), for a given precipitation (P)). Thus, the stable state with vegetation might be caused and stabilised by a positive feedback between vegetation and local precipitation. If the initial vegetation is low the positive feedback loop will work vice versa. So, the vegetation declines and the system collapses to a degraded state (taken from Kéfi (2008)).

physically based modelling (Wheater et al., 2008). In recent years, there has been a wide assortment of research on modelling vegetation pattern formation and vegetation-water dynamics on drylands (e.g. Thiery et al. (1995); Ludwig et al. (1999); HilleRisLambers et al. (2001); Tongway and Ludwig (2001); Rietkerk et al. (2002); Porporato et al. (2003); Fernandez-Illescas and Rodriguez-Iturbe (2004); Gilad et al. (2004); Meron et al. (2004); Boer and Puigdefábregas (2005); Saco et al. (2007); Pelletier et al. (2012)). Commonly, band formation and patterned vegetation are mathematically obtained with reaction-diffusion equations for vegetation biomass and water availability (Borgogno et al., 2009). An outstanding review of ecohydrological models of vegetation pattern formation is found in Borgogno et al. (2009), who provide a rigorous analysis of the

major theories explaining the mechanisms underlying such landform-vegetation pattern formation. Constructively, recent modelling studies have focused on the interactions between water redistribution and vegetation patterns by giving important insight into structural transformations on a mechanistic level (e.g. HilleRisLambers et al. (2001); Rietkerk et al. (2002)); nonetheless they do not encompass landform-water-vegetation feedbacks (Saco and Moreno-de las Heras, 2013).

Of the numerous published studies that have modelled vegetation band development, we solely centre on the approach by Saco et al. (2007), who first pointed out the importance of topography in controlling banded vegetation systems utilising a modelling framework. They investigated the interaction between dynamic vegetation patterns and geomorphology in banded vegetation systems, deploying a coupled, dynamic vegetation-landform evolution model. They looked at the interactions between patterned vegetation and erosion by accounting for the effect of dynamic water redistribution. The authors utilised a dynamic vegetation model for the development of vegetation pattern in water limited ecosystems that describes the dynamics of three state variables: plant biomass density, soil moisture, and overland flow. In addition, they used SIBERIA (Willgoose et al., 1991), a physically based model of the evolution of landforms under the action of fluvial erosion, creep and mass movement. Their model reproduced vegetation patterns, as obtained by other models of arid ecosystem dynamics, and a stepped microtopography, as observed in the field.

Saco and co-workers found that stationary and migrating vegetation bands self-organise perpendicular to the flow direction and their appearance is associated with emergence of a runon-runoff pattern. Seed dispersal might be preferentially oriented in the downslope direction owing to transport in runoff. Banded vegetation arises on hillslopes where water flow is disrupted by bands of vegetation resulting in facilitation due to increased water availability in these areas, whereas water availability is lower in inter-band areas thus inhibiting vegetation growth.

The erosion-deposition mechanisms change microtopography, influencing surface water redistribution, soil moisture spatial patterns and the evolution of the vegetation patterns (Saco et al., 2007). This has a major effect on the co-evolution of biotic (i.e., ecosystem, community, population, individuals) and abiotic (i.e., region, catchment, hillslope, soil patch) units (Saco et al., 2007).

Chapter 3

Methods

The theme of this chapter is on describing the ways in which we address the research questions posed in the introduction (chapter 1). We select to utilise a two-dimensional simple lumped model (Karssenberg, 2014), which is derived from a fully-distributed process-based hillslope evolution model (Karssenberg, 2011). It is basically devised to describe the interaction between the vegetation and the soil subsystem. It should be noted that we solely give a brief and to the point description of these models here, in view of the fact that they have been fully described elsewhere.

3.1 Models description

3.1.1 Distributed model

A fully-distributed model – parameters, inputs and outputs vary spatially – of an $80m$ by $40m$ hillslope (figure 3.1b) simulates the evolution of a semi-arid vegetation-soil system over hundreds of years with a weekly time step containing a shift from a vegetated hillslope with thick soils to a hillslope with low vegetation cover and degraded soils. Figure 3.1 (a) shows a causal loop diagram illustrating the key positive (+) and negative (-) effects of the system.

Water enters the system via rainfall and exits from it via evapotranspiration and surface runoff. Each week either zero or one rainfall events occur. This is determined by drawing from a discrete probability distribution. The water on the ground surface enters the soil up to the maximum infiltration capacity or until the soil has reached its maximum water content. Evapotranspiration is modelled as a function of the vegetation biomass.

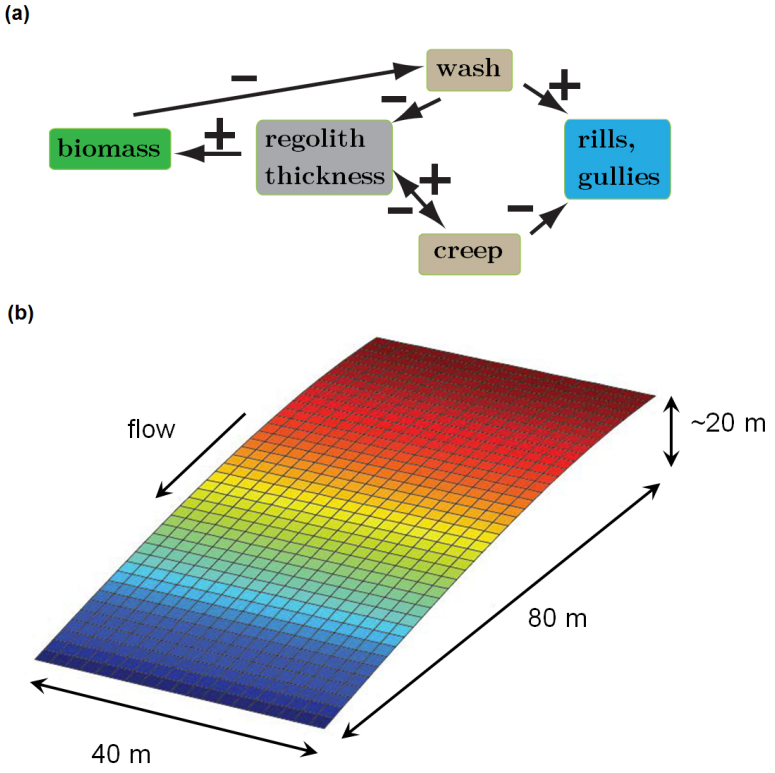

FIGURE 3.1: (a) Casual loop diagram depicting the positive and negative feedback loops in the modelled system (taken from Karssenberg (2011)). (b) The model area: a hillslope with length and width of 40 m and 80 m respectively (Karssenberg et al., 2015).

Considering two well-studied ecological model systems of vegetation collapse in semi-arid regions (Noy-Meir, 1975; May, 1977), vegetation biomass grows logistically including spatial diffusion of biomass. The vegetation cover is calculated as a function of grazing pressure, soil depth and hydrology. Regolith (soil) thickness is modelled by soil creep and wash processes (i.e., erosion by wash and splash), as a function of rainwater reaching the ground surface and runoff. Vegetation growth rate depends on regolith thickness and soil wash is inversely proportional to the vegetation cover. The main output of the model is a time series of hillslope geometries such as topographical surface, development of gullies, regolith thickness, and vegetation coverage. For a detailed description of the distributed model, refer to Karssenberg et al. (2015).

3.1.2 Lumped model

3.1.2.1 Representing the change in soil depth and vegetation biomass

An appropriate representation of the key processes of the system is provided by a simple lumped model which consists of a set of two coupled differential equations describing the dynamics of soil and vegetation subsystems. The equations and parameters of the

lumped model are derived from the aforementioned distributed model (Karssenberg et al., 2015). The change in the soil depth is determined by bedrock weathering and net erosion, and the change in biomass is determined by vegetation growth and grazing terms.

The change in soil depth D (m) is modelled as:

$$\frac{dD}{dt} = W_0 e^{-aD} - e^{-B/b}(E_t + e^{-D/c}(E_0 - E_t)) - C + e \tag{3.1}$$

Soil thickness is dependent on the balance between soil production and erosion. In equation 3.1, the first rhs (right-hand side) term corresponds to soil production function. The rate of weathering of bedrock can be modelled as an exponential reduction with thickening of the soil, with W_0 the potential soil production rate occurring under zero soil depth and a an empirical constant (weathering exponent).

The second rhs term stands for water erosion and the third rhs term is the soil loss by downhill creep. Concerning soil erosion by water processes, a decrease in soil depth increases erosion in the wake of the lessened maximum soil water content. In this way, the soil becomes saturated resulting in increased surface runoff. To represent this effect of soil depth on erosion, the erosion rate parameter E_0 and the exponent c are used. Also, note that E_t stands for erosion rate at zero biomass and an infinitely thick soil layer. A possible increase in biomass vegetation maintains slopes and reduces erosion owing to increased intercepted rainwater and infiltration capacity of the soil that tends to go up, holding more rainwater on-site and decreasing runoff. Exponent b corresponds to this influence of biomass on erosion.

The last term, e, corresponds to a Gaussian noise process representing environmental stochasticity, which is added to the deterministic processes in order to be in a position to detect the early warning signals. We expand a bit further on this at the end of the current chapter.

The change in biomass B (kg/m^2) is modelled as:

$$\frac{dB}{dt} = (1 - (1 - i)e^{-D/d}) \left(rB \left(1 - \frac{B}{c} \right) \right) - g \left(\frac{B}{s + B} \right) + e \tag{3.2}$$

In equation 3.2, the first rhs term stands for the growth of the vegetation and the second rhs one represents its consumption by grazers. The first part of the first rhs term describes the decline in growth rate when soil depth decreases, with the exponent d and the intercept i. Additionally, the second bit of the first rhs term corresponds to a well-studied overharvesting model system of vegetation collapse which has been regularly

used in investigating dynamics of critical transitions (Noy-Meir, 1975; May, 1977). The grazing term (second term) incorporates the grazing pressure g, whose influence can lead to bistable dynamics. As with the soil depth, some random noise e is added.

The primary driver of the system is the grazing pressure, which, when going up, is consequent on decrease in environmental compartments such as soil thickness and vegetation biomass, leading to the occurrence of a critical transition. A succinct description of various parameters and symbols is available in the following subsection 3.1.2.3.

Bear in mind that the identification of parameters in the above differential equations has been done by manual calibration. A good fit between the rates of change computed by the lumped model and those computed by the distributed model, has been obtained, where the system has been on the brink of crossing the catastrophic shift. Parameters have been adjusted, specifically resulting in an adequate fit between soil thickness and biomass values, utilising a good many combinations of soil thickness and biomass values. For a more complete account of this procedure, refer to Karssenberg et al. (2015).

3.1.2.2 Stability and steady-state solution

As discussed previously, stability of an equilibrium has a reference to the system propensity to get back to its former position after a perturbation. Here, the dynamic equilibrium of the system (i.e., the system does not change anymore) is found by setting the rate of change equal to 0 (equation 3.3; 3.4) and solving the resulting algebraic equations (see appendix B).

$$\frac{dD}{dt} = f(D) = 0 \qquad (3.3) \qquad\qquad \frac{dB}{dt} = f(B) = 0 \qquad (3.4)$$

As another option, the equilibrium point can also be found by running the model dynamically for a sufficiently long time. In this case, the model succeeds in obtaining the steady state situation by itself, running until it stabilises.

The steady state for both soil and vegetation subsystems can be graphically represented by the crossing of the stable equilibria lines (red dot in the figure 3.2). Under increasing of grazing pressure g, the system is held at equilibrium as late as the equilibria lines for vegetation and soil intersect. On this account, when these lines stop being crossed, the system undergoes a critical transition towards a bare state (i.e., biomass and soil depth is around zero).

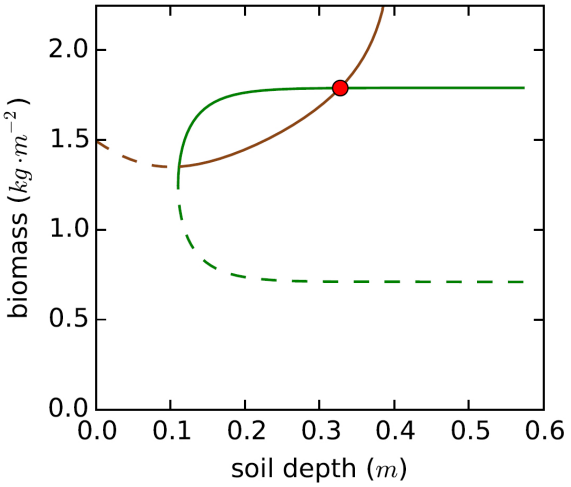

FIGURE 3.2: Stability diagram of the lumped model. The green line corresponds to the vegetation subsystem and the brown line represents the soil subsystem (solid branches of the curve, stable equilibrium; dashed branches, unstable equilibrium). The two subsystems are in equilibrium at the location where the stable equilibria lines cross, shown by red round.

3.1.2.3 Parameter values used for the simulations

The inputs and parameters of the lumped model representing the soil and vegetation changes, are explicitly summarised in the following table 3.1. We considered the same parameter values set as in Karssenberg (2014).

Symbol in the text	Parameter in the script	Value	Unit	Explanation
parameters in soil depth model				
W_0	w	0.0005*	m/y	Soil production rate as a result of bedrock weathering for bare bedrock (D=0)
α	e	4.0*	m^{-1}	Weathering exponent parameter
D	r	0.4*	m	Soil thickness
$1/c$	p	20	m^{-1}	Exponent related to the effect of soil depth on erosion
E_0	z	0.084	m/y	Erosion rate for soils without soil cover
E_t	m	0.021	m/y	Erosion rate for soils with infinite soil cover
B	b	1.0*	kg/m^2	Biomass
b	v	0.28	m^{-1}	Exponent related to the effect of biomass on erosion
C	c	0.0001	m/y	Soil loss by creep
parameters in biomass model				
D	r	0.4	m	Soil thickness
d	a	0.04	m^{-1}	Regolith range

i	i	-0.7		Regolith intercept
r	g	2.1	y^{-1}	Growth rate
B	b	1.0	kg/m^2	Biomass
c	c	2.9	kg/m^{-2}	Carrying capacity
g	s	1.75*	$kg\,m^{-2}\,y^{-1}$	Grazing pressure
s	s	0.4	kg/m^2	Vegetation density
e	e	0.2 %		SD of Gaussian noise

TABLE 3.1: Listing of the various symbols along with values used in this study. Values marked with a star symbol (*) correspond to the initial ones.

3.2 Model scenarios

Following Karssenberg (2014), we considered two main model scenarios concerning the impact of soil parameters on the transient behaviour of the system – one with low and one with high bedrock weathering rates. In particular, in these two scenarios the values for bare bedrock weathering rate W_0 and the weathering exponent parameter a were tuned, as shown in table 3.2. The ensuing parameter values for soil thickness D and biomass B are given as well.

We ran the model for different combinations of the initial values of state variables. Note that the grazing pressure g was set just above the respective threshold values when the shift was reached, and kept fixed after that. We refer to these scenarios as low and high bare bedrock weathering rate scenarios. Using as a basis these scenarios, the transient responses in the course of critical transition in our system are analysed, with specific interest on the identification of early warning signals.

	Low bare bedrock weathering rate scenario	High bare bedrock weathering rate scenario
Soil production rate as a result of bedrock weathering for bare bedrock (W_0) (m/y)	0.0004	0.002
Weathering exponent parameter (α) (m^{-1})	3.47	7.49
Soil thickness (D) (m)	0.20	0.25
Biomass (B) (kg/m^2)	1.50	1.22
Grazing pressure (g) (kg/m^{-2})	1.9390	1.9660

TABLE 3.2: Parameter values for the two different scenarios (i.e., low and high bare bedrock weathering rates).

3.3 Model analysis

The analysis of the output of the model is mainly based on the diagnostic indices which are suggested as precursors to the catastrophic regime shifts. Our goal here is to develop, evaluate and contrast the different early waning signals by measuring the magnitude of changes in the statistical properties (i.e., alterations in variability) of the time series produced by the lumped model. To this end, we straightforwardly calculated the following potential indicators for the simulation results.

3.3.1 Calculating early warning signals

Variance

When the system is nearing a tipping point, the return time to equilibrium upon a slight perturbation comes to be pretty small (i.e., critical slowing down). In consequence of this, the variance of fluctuations in state variables (e.g. biomass and soil thickness) may discernibly change (increase or decrease) over time. It therefore can serve as an early warning. Variance, or second moment about the mean μ of a distribution, can be estimated by the following mathematical formula:

$$V = \frac{1}{n-1}\sum_{i=1}^{n}|x_i - \mu|^2 \tag{3.5}$$

where x is the state variable value and μ is the mean value of x.

Skewness

Apart from the variance, a system approaching a regime shift can experience an increase in the asymmetry of the fluctuations and this does not ensue from critical slowing down (Guttal and Jayaprakash, 2008). Importantly, in the same way as variance, we may observe an increase in skewness of the distribution of states. More generally, it might either increase or decrease, turning upon whether the shift is towards a contrasting state that is larger or smaller than the present state (Dakos et al., 2012). Skewness, symbolised by SK, is a pure number (i.e., nondimensional) measuring the degree of asymmetry and it can be estimated as the third moment around the mean:

$$SK = \frac{\frac{1}{n}\sum_{i=1}^{n}(x_i - \mu)^3}{(\sqrt{\frac{1}{n}\sum_{i=1}^{n}(x_i - \mu)^2})^3} \tag{3.6}$$

where x is the state variable value and μ is the mean value.

Basically, we are interested in investigating how quickly the catastrophic regime shift unfolds and importantly, whether the selected early indicators provide sufficient advance warning in such a mixed system composed by a slow and a fast subsystem.

Seeing that we perform a transient simulation, model simulations start with grazing pressure g just below the critical value where the transition occurs. We then increased it, little by little, until reaching the point of the shift, and then kept it constant during the system collapse shortly or long afterwards, depending on the response time of the system (i.e., the pace of response).

The dryland ecosystem is always perturbed in the sense that it is always in a stochastic environment of perturbations. We mean to say that the state of the system may well fluctuate over time. When the system is on the brink of crossing the critical point, the manner of how it fluctuates changes by rule, enabling us to detect generic indicators. In this respect, to be able to foresee the critical shift, we included stochastic dynamics in the model. This can be done either by adding some Gaussian random noise (i.e., statistical noise which conforms to a Gaussian probability density function) on the grazing pressure g or as additive directly to the state variables.

Here, we assume that a repeated, normally distributed noise is independently added to the biomass and the soil thickness stepwise (i.e., every week). More specifically, we generated a noise process that takes random values from a normal distribution with a mean equal to zero and 0.2% standard deviation of the biomass or soil thickness in the dynamic section of the model over a set of time steps. Note that the amount of noise was kept the same over time.

The above process permits us to capture the statistical signatures of the dynamic effect of our system (i.e., the phenomenon of critical slowing down) that becomes apparent in the vicinity of tipping points. Estimations of leading indicators (variance, skewness) were done utilising PYTHON's pandas data analysis toolkit. We applied rolling statistics functions on biomass and soil depth time series within moving windows of fixed size. The window size in weeks was chosen in such a way to track the variation and simultaneously not to be excessively large; this depends of course on how quickly the system is collapsing. This is to say that when the regime shift unfolds at a slow pace, the system change is so little that we could perhaps have used a bigger window size.

Our analysis, at its most basic level focuses on the temporal indicators that presage the approaching shift. We set side by side the search for indicators that typically predict the advance on critical point inferring a quick transition and the potential warning signals

that may additionally arise in a much more gradually collapse, after crossing the tipping point.

All simulations and statistical analyses are performed in ENTHOUGHT CANOPY v.1.3.0 (`https://www.enthought.com/products/canopy/`) using a combination of the PYTHON v.2.7.6 (`https://www.python.org/`) and PCRaster 4.0.0 (freely available at `http://pcraster.geo.uu.nl/pcraster-4-0-0/`) scripting language.

Chapter 4

Results

In what follows, we present the results of the processes described in the previous chapter 3. The time series of the lumped model are analysed by putting to the test different values of soil parameters and estimating the statistical indices, giving attention to their behaviour prior to, as well as after the critical point where the system starts collapsing.

4.1 Model behaviour

4.1.1 Equilibrium point and stability

Let us set about the current section by inspecting the stability of the lumped model performing a graphical investigation of the steady-state behaviour. The equilibrium state (i.e., the stable fixed point of the model) is obtained where the rate of change of the two state variables is synchronously zero, as a function of their values ($dD/dt = 0$ and $dB/dt = 0$).

By plotting the resulting equilibrium lines, a graphical representation of the steady-state and stability conditions of the lumped model can be seen in figure 4.1. Stability graphs for the vegetation (green line) and the soil (brown line) subsystems are presented on the left-hand side panels of the figure. On the right, depicted is the direction and the rate of change of the two state variables. Where the two isoclines intersect, both subsystems are in dynamic equilibrium (i.e., sources and sinks are in balance), indicated by the red dot (figure 4.1). This means that the system will go back towards the equilibrium when it is slightly perturbed from it. Now then, if it is considerably displaced from the equilibrium, consequently it will collapse to the contrasting state. This happens when the system state drops either below approximately 0.1 m soil depth or 0.6 kg/m^2 vegetation biomass.

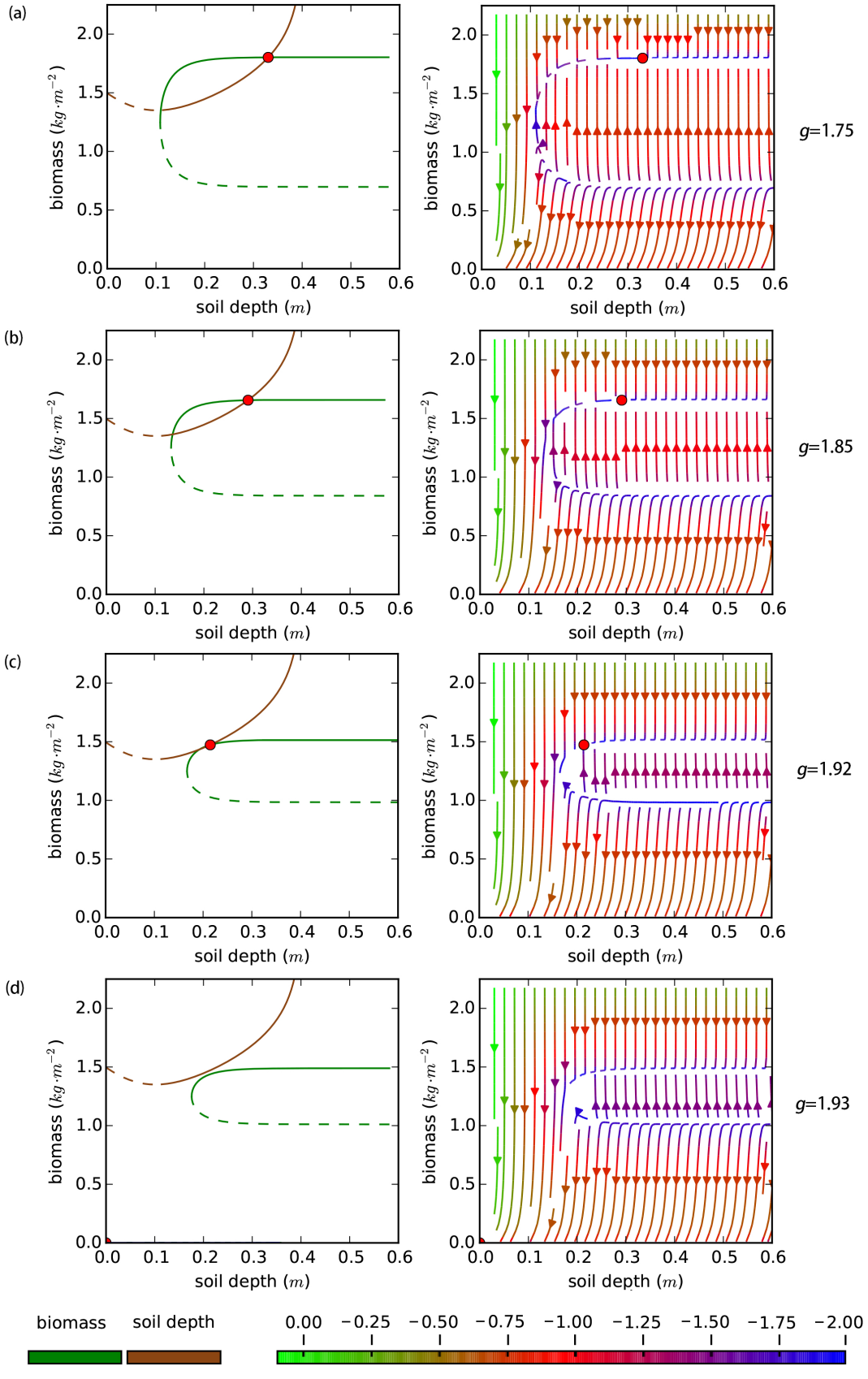
(a)
(b)
(c)
(d)
biomass ($kg \cdot m^{-2}$)
soil depth (m)
0.0 0.1 0.2 0.3 0.4 0.5 0.6
0.0 0.5 1.0 1.5 2.0
g=1.75
g=1.85
g=1.92
g=1.93
biomass
soil depth
0.00 −0.25 −0.50 −0.75 −1.00 −1.25 −1.50 −1.75 −2.00

The dynamics of our system depend on the driving variable (i.e., grazing). With increasing grazing rate g, the equilibrium line for vegetation seems to move towards lower biomass and higher soil thickness values; the equilibrium point (red round) changes position downwards, throughout the length of soil equilibrium line (figure 4.1 panel a to panel d). The different levels of grazing rates presented here correspond to g= 1.75, 1.85, 1.92 and 1.93 $kg \cdot m^{-2} \cdot w^{-1}$.

4.2 Scenario analysis

In figure 4.2, one can see the system's response for both scenarios from a state at which the critical threshold is just exceeded to a new equilibrium state corresponding to a full collapse. Additionally, the panels in figure 4.3 represent the stability diagrams of the model for each of these scenarios at level of grazing parameters where the system undergoes a critical transition.

We first touch on the results of low bedrock weathering rate model scenario (W_0=0.0004, a=3.47) in which the grazing pressure rate is held constant, just above the critical value at g=1.9390 $kg \cdot m^{-2} \cdot w^{-1}$. As it can be seen in figure 4.2, the system exhibits a long-lasting transient response. In particular, the transition unwinds within approximately 260 years. Soil thickness reduces with heavy steps along with vegetation biomass. Then, in about 200 years, the vegetation subsystem starts responding in a much quicker manner and eventually collapses. Once it has completely collapsed, soil depth drastically diminishes towards zero.

By contrast, when increasing the bare bed weathering rate values – high bedrock weathering rate scenario (W_0=0.002, a=7.49) – a sharp, rapid transition from one state to another can occur, happening in a span of decades (figure 4.2). In this case, the protracted transient time period corresponding to the previous setting cannot be seen any longer. The soil subsystem starts slowly declining and steeply collapses straight away in the time following the ultimate vegetation collapse. Note that here the grazing parameter value is set at g=1.9660 $kg \cdot m^{-2} \cdot w^{-1}$.

FIGURE 4.1 *(preceding page)*: Left, stability diagrams of the lumped model. The vegetation subsystem is represented by the green line and the soil subsystem by the line in brown colour. The solid lines symbolise stable equilibria, whereas the broken lines correspond to unstable equilibria. The two subsystems are in equilibrium at the location where the stable equilibria lines cross, shown by the red dot. Right, the rate of change for the lumped model. The arrowed lines point towards the direction of change; colour scale represents log-transformed values. An increase in grazing rate moves the fixed point downward from panel to panel. When the two stable equilibrium lines come to be separated the system goes through a critical shift (d).

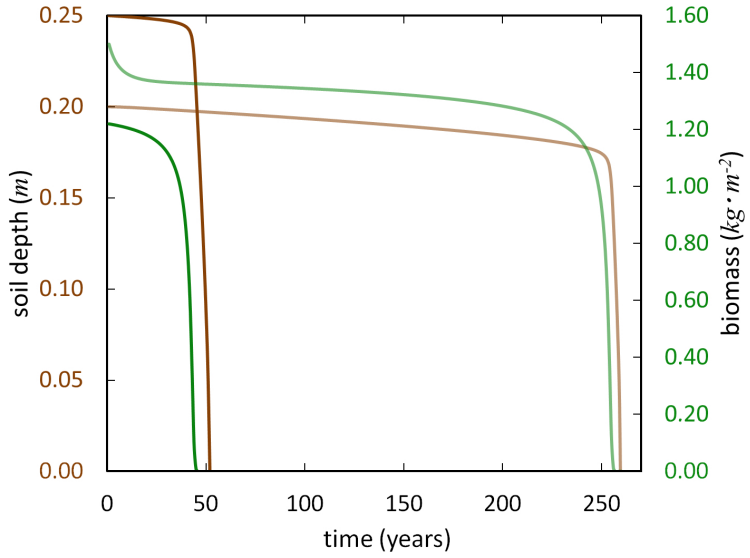

FIGURE 4.2: The unfolding of the catastrophic regime shift (green lines, biomass; brown lines, soil thickness). The pale-coloured lines correspond to low bare bedrock weathering rate values and the deep-coloured lines represent the high bare bedrock weathering rate scenario.

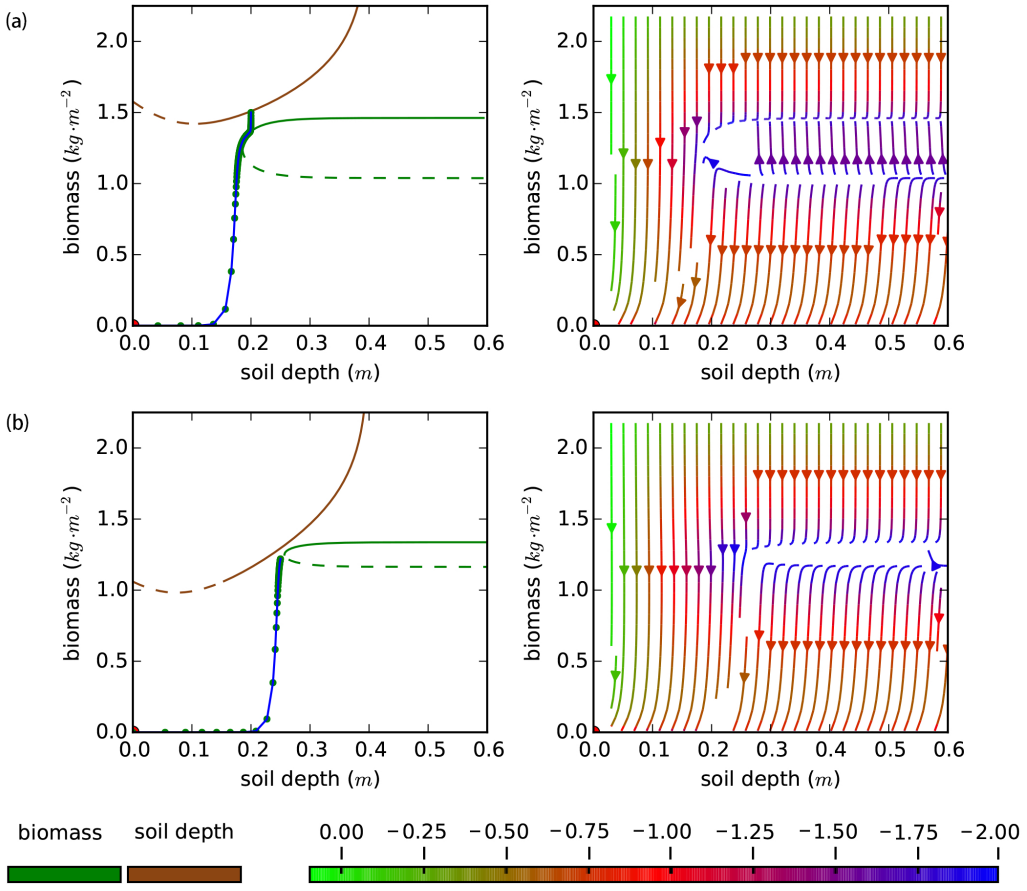

FIGURE 4.3: Regime shift. Stability plots for (a) low bare bedrock weathering scenario and (b) high bare bedrock weathering scenario with grazing pressure g just above the threshold value where the transition occurs (green lines, biomass; brown lines, soil thickness). The solid lines represent the stable equilibria and the dashed lines correspond to the unstable equilibria. The blue line represents the transient response between the two alternative stable states (green round marks symbolise years). The panels on the right-hand side show the rate of change. The arrowed lines point towards the direction of change; colour scale represents log transformed values.

Thus, it can be clearly observed that changes in the soil parameters, and more specifically, the altering of bare bedrock weathering rate values, have a considerable effect on the transition time after a threshold has been transgressed (high W_0 scenario, takes around 50y; low W_0 scenario, takes around 260y).

This difference is due to the fact that the position of stable equilibrium lines of the system change in each scenario model run. In particular, for the scenario with high bare bedrock weathering the equilibrium line of soil thickness is placed less high in position corresponding to lower biomass values than the soil equilibrium line in the low bare bedrock scenario (figure 4.3).

4.3 Early warning indicators

4.3.1 Low bare bedrock weathering rate scenario (slow response)

We consider the case that the system exhibits a slow, transient response. A single realisation of this model scenario is presented below, showing the simulated dataset of biomass and soil thickness (figure 4.4 and 4.5 respectively). Beginning simulations from equilibrium, the level of grazing pressure is initially set to g=1.0 $kg \cdot m^{-2} \cdot w^{-1}$. Then, it very slowly increases in a linear manner stepwise (i.e., $6.8 \cdot 10^{-6}$ units every week), until it reaches a critical value ($g \approx 1.90$ at $t \approx 2500$), and is kept constant thereafter while the system is already in a transient state. Although the gradual increase of grazing rate, the system remains in the vegetated state for 2540 time units. After that time, the regime shift unrolls over a span of 1000 years, a relatively long period of time given that typically, ecosystems on the brink of crossing a critical threshold shift pretty sharply to alternative states.

Both biomass and the soil thickness time series fluctuate randomly in reaction to the additive noise at each time step. On approaching the transition point, the variability on the vegetation time series visibly increases (figure 4.4). This random variation seems to slightly increase further just before the actual moment of the collapse (figure 4.4). As regards the soil time series, we cannot observe such a visible change in random variation as the transition is approached (figure 4.5).

Delving into these qualitative features, we consider the probability distribution of a snapshot of the dynamical variables of the model when the system is far from (g= 1.59), and near to (g=1.89) the critical point (figure 4.6). At g= 1.59, the probability density of biomass time series appears to be symmetric and with a relatively tight distribution span. Near the switch point, the histogram becomes wider and looks to be developing

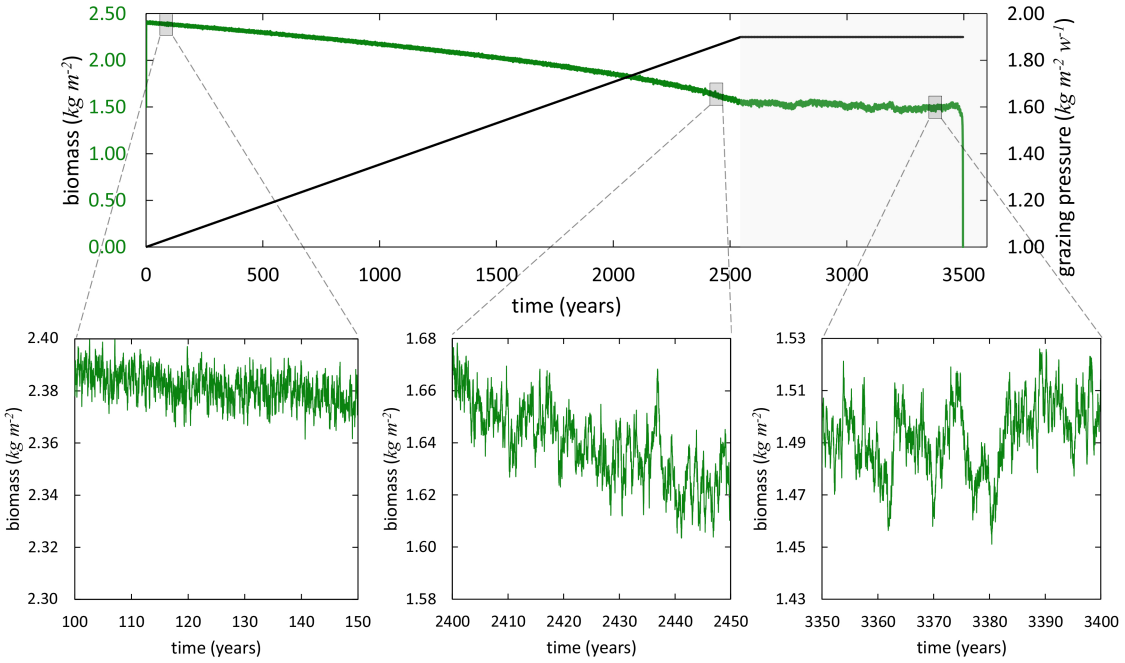

FIGURE 4.4: Slowly unfolding regime shift. Time series of biomass (green line). The gradual increase of grazing rate (black line) brings about a slight decrease in biomass until a critical point is reached beyond which the regime shift starts unfolding (transparent grey rectangle region). The lower plots zoom in on a much finer time scale showing the variation in biomass when the system is, far from the transition (t=100-150; left), prior to the critical threshold (t=2400-2450; in the middle) and before the actual moment of transition (t=3350-3400; right).

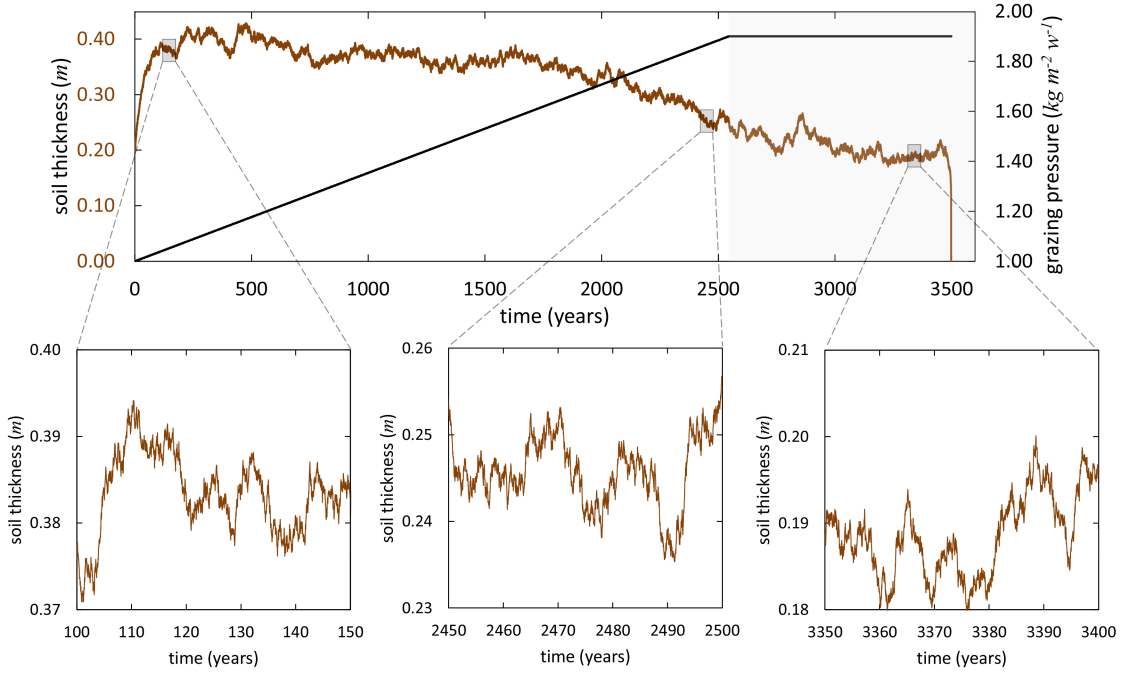

FIGURE 4.5: Slowly unfolding regime shift. Time series of soil thickness (brown line). The gradual increase in grazing pressure (black line) drives the system slowly to a catastrophic collapse (transparent grey rectangle region), with bottom panels zoomed in far from the transition (t=100-150; left), prior to the critical threshold (t=2450-2500; in the middle) and before the actual moment of transition (t=3350-3400; right).

an asymmetric tail to the left (i.e., negative skewness). Further, no considerable asymmetry in the distribution of soil depth is observed, in view of the fact that changes of variability in soil thickness time series has not been observed either (e.g. figure 4.5). These characteristics set the basis for the early warning indicators proposed below. Note that extra plots of these simulations can be found in the Appendix A (figure $A.2$).

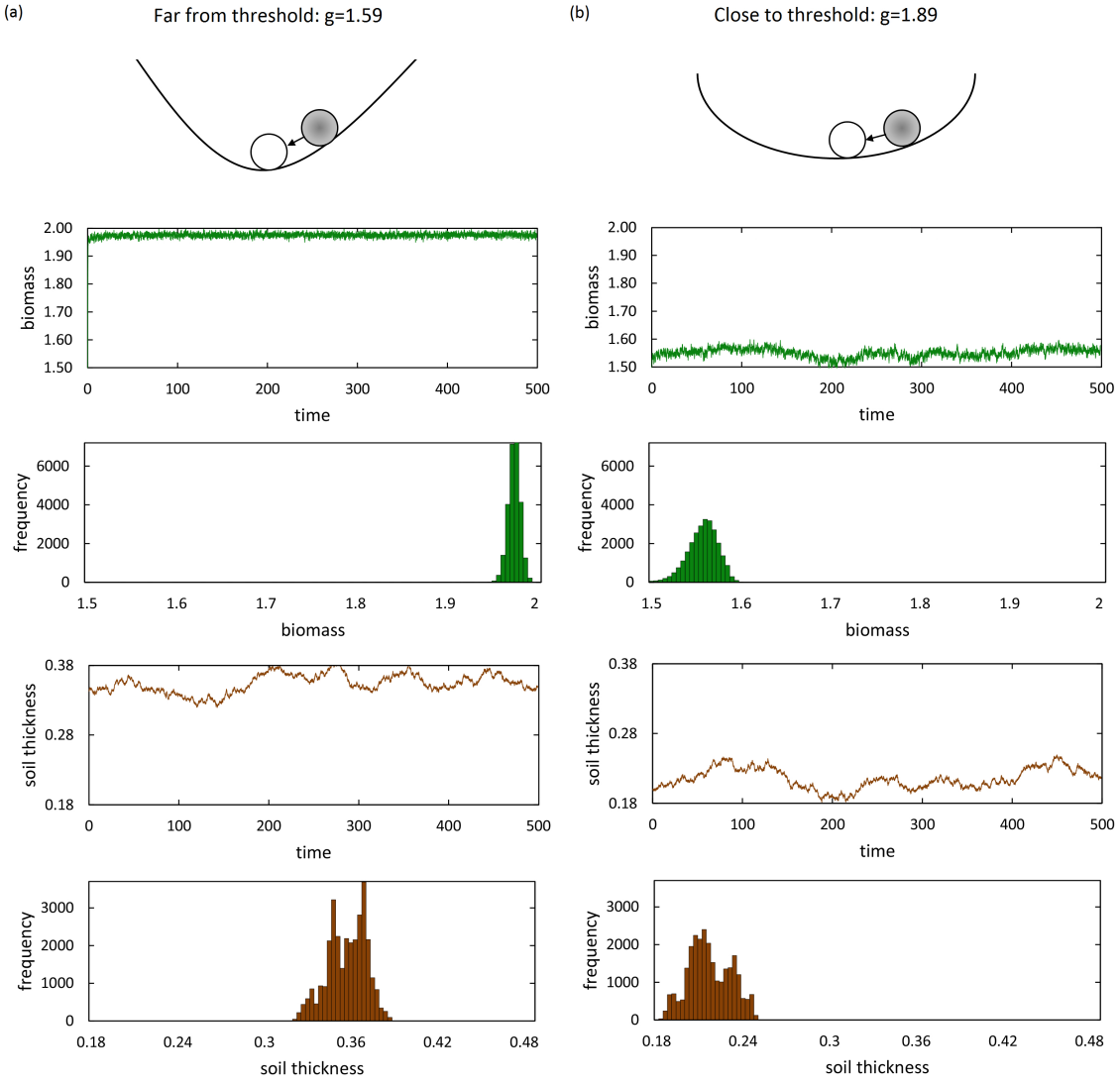

FIGURE 4.6: Figure displaying the qualitative behaviour of the state variables as the system gets closer to the threshold of collapse. This can be shown intuitively by the landscape illustration at the top of the figure. The numerical simulation results for biomass (green) and soil thickness (brown) time series and their probability density (histograms) based on static grazing rates when the system is far from (g=1.59; left-hand side) and close to (g=1.89; right-hand side) the critical threshold.

4.3.1.1 Variance and skewness

We estimate the leading indicators (i.e., variance and skewness) applying a moving window of 200 years. On the biomass time series, variance substantially increases prior

to the transition point (figure 4.7b; left). It also roughly rises toward the actual collapse, though exhibiting a relatively strong variation (figure 4.7b; right). Moreover, skewness decreases showing a peak just before the switch point (figure 4.7c; left), whereas no evident change is observed after the onset of the shift (figure 4.7c; right). Concerning the soil depth, we find no apparent change signalling the critical shift. When plotting the statistical indices over time, noisy erratic trends for both variance and skewness are observed (figure 4.8).

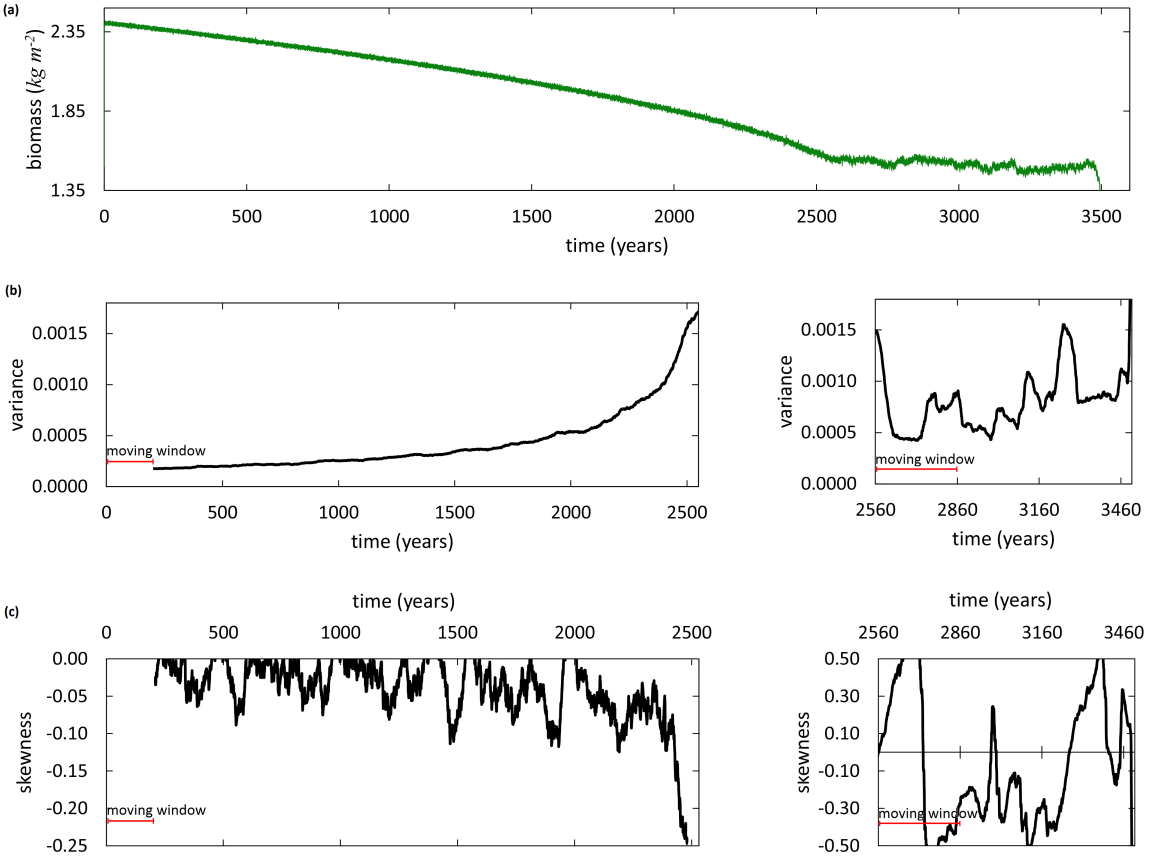

FIGURE 4.7: (a) Time series of biomass. Quantitative measures of variability of the time series: (b) variance and (c) skewness of biomass estimated within moving window of size 6% of the time series; right-hand side panels show the time period after the transition point is passed.

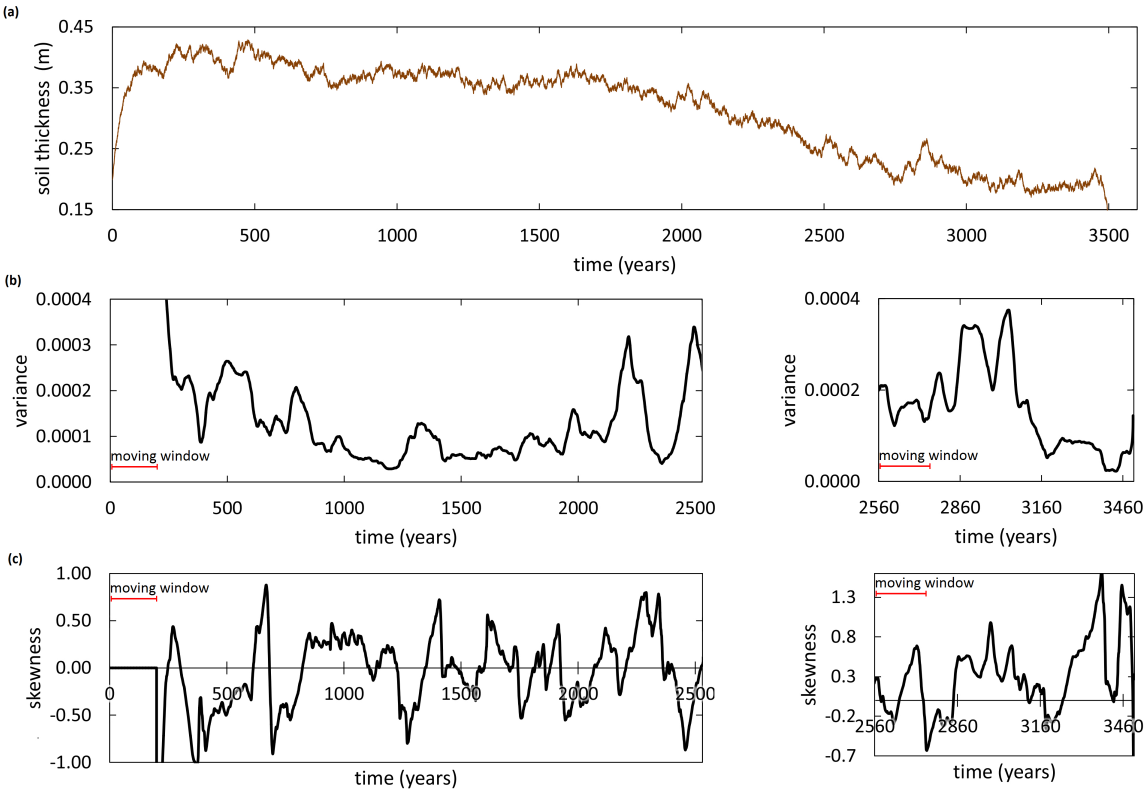

FIGURE 4.8: (a) Time series of soil thickness. Quantitative measures of variability of the time series: (b) variance and (c) skewness of soil thickness estimated within moving window of size 6% of the time series; right-hand side panels show the time period after the transition point is passed.

4.3.2 High bare bedrock weathering rate scenario (fast response)

In contrast to the aforementioned model scenario, we now consider the case where the system typically undergoes a direct, rapid transition. The simulation results can be seen in figure 4.9 (biomass time series) and 4.10 (soil time series). As in the other scenario, simulation started with system in the vegetated stable state, and progressively increasing the grazing rate at a slow pace (i.e., $7 \cdot 10^{-5}$ units every week) from g=1.0 to g=1.97 (critical value). Once this threshold is crossed (g$\approx$ 1.97 at t$\approx$ 270), grazing rate stops increasing and the system quickly jumps to the degraded state.

The critical transition occurs at t$\approx$270y where the system precipitously switches to the unvegetated state. Similarly to the earlier subsection, the fluctuation in biomass gets greater in the direction of the shift (figure 4.9), whilst the variation in the soil does not (figure 4.10). If we now look at the frequency distributions we find analogous results. At low levels of g, the histogram of biomass has a symmetric shape characterised by small width, whereas nearing the critical threshold, the distribution widens out tending to have a tail to the left (i.e., negative skewness) (figure 4.11).

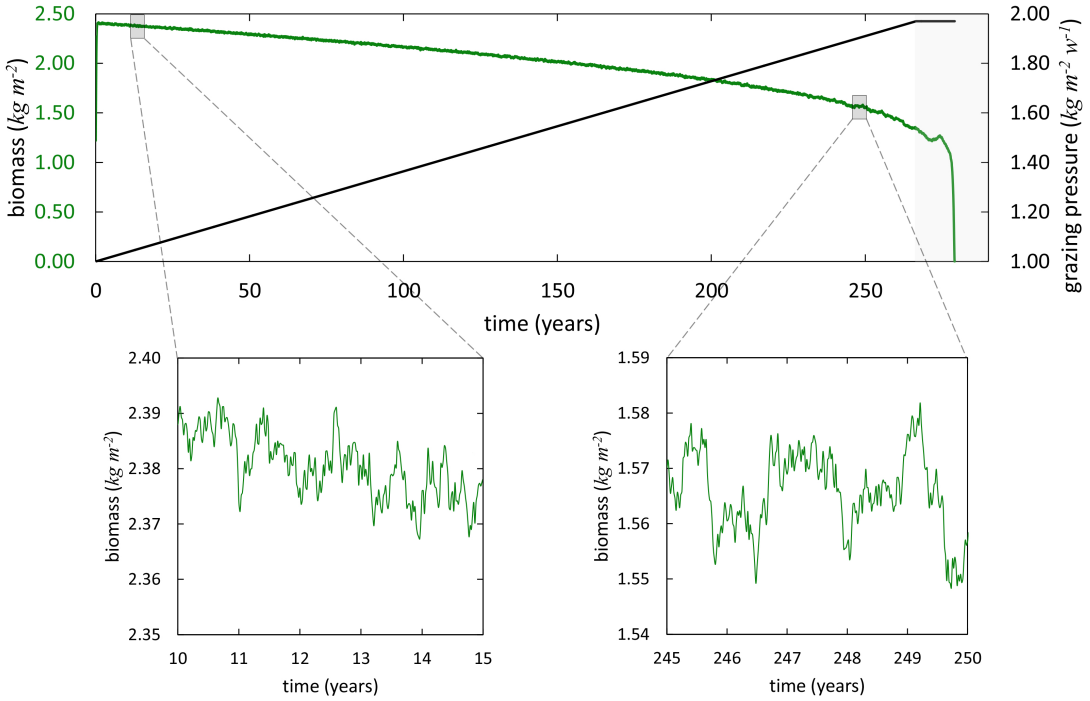

FIGURE 4.9: Quickly unfolding regime shift. With the slow, linear increase of grazing rate (black line) over time, biomass (green line) gradually declines through time until it nears a critical point at which the system starts collapsing (transparent grey rectangle region). The plots at the bottom of the panel zoom in on a much finer time scale (i.e., 260 time steps) showing the difference in biomass variation on the time series far from the transition (t=10-15; left-hand side), and toward to the critical threshold (t=245-250; right-hand side).

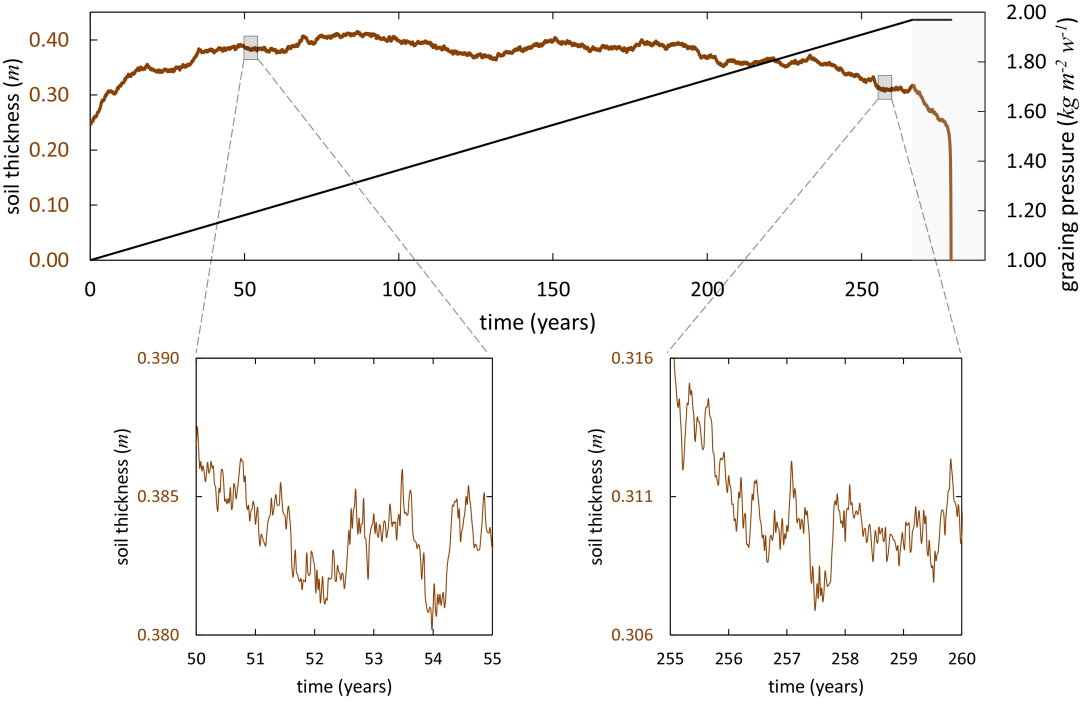

FIGURE 4.10: Quickly unfolding regime shift. Time series of soil thickness (brown line). Grazing pressure (black line) linearly increases over time causing a critical transition (transparent grey rectangle region).

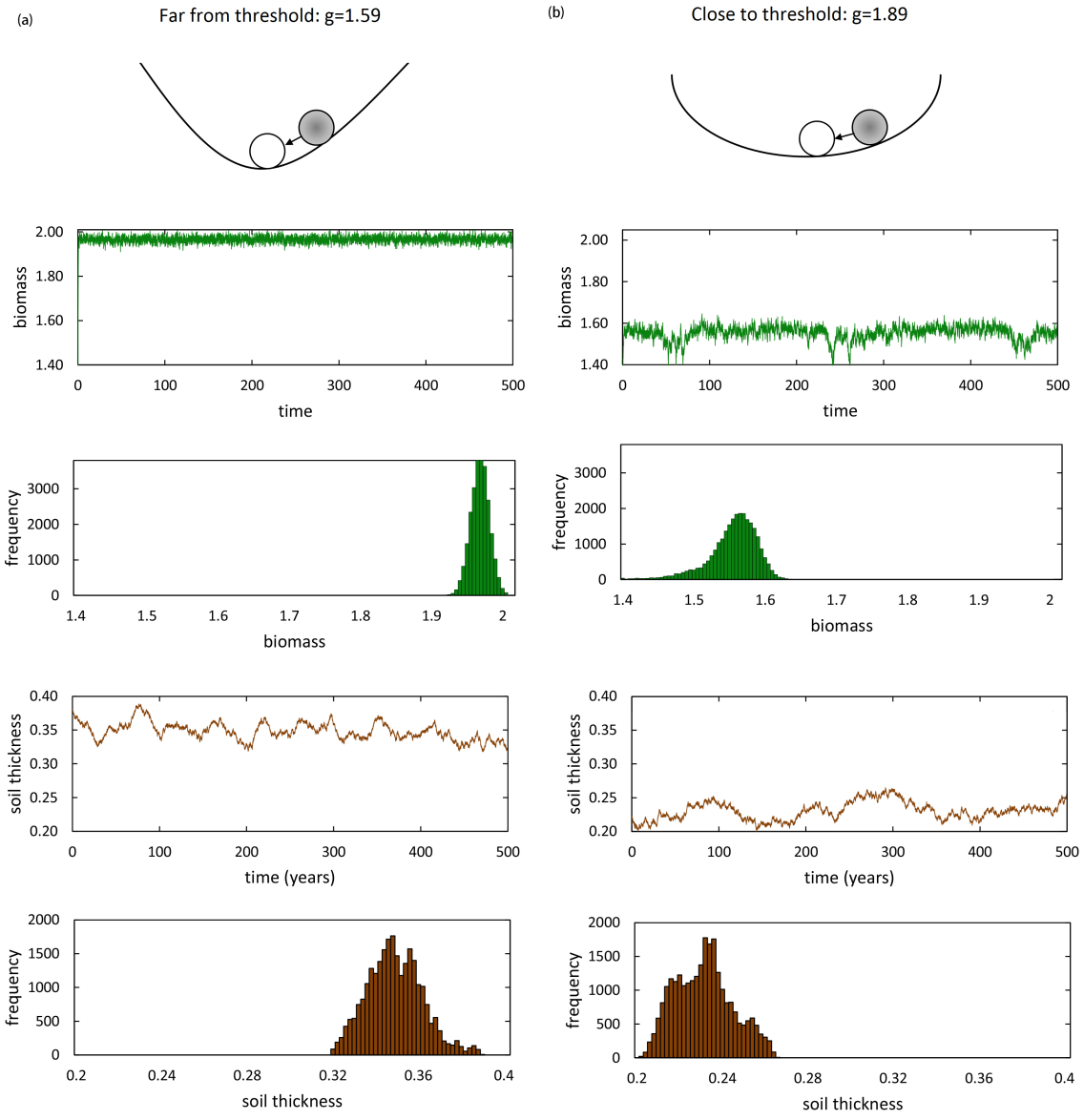

FIGURE 4.11: Figure displaying the qualitative behaviour of the state variables as the system gets closer to the threshold of collapse. This can be shown intuitively by the landscape illustration at the top of the figure. The numerical simulation results for biomass (green) and soil thickness (brown) time series and their probability density (histograms) based on static grazing rates when the system is far from (g=1.59; left-hand side) and close to (g=1.89; right-hand side) the critical threshold.

4.3.2.1 Variance and skewness

Once more, we estimate the higher-order statistics applying a moving window of 10% of the time series (window size= 30 years). Regarding biomass time series data, variance clearly shows an upward trend well ahead of the shift (figure 4.12b). In an analogous fashion, skewness declines, peaking when the system is on the brink of crossing the critical point (figure 4.12c). Accordingly, these characteristic trends clearly provide

indication of the nearby systemic transition. Our simulations also show that no early warning signals were found in soil thickness time series (figure 4.13).

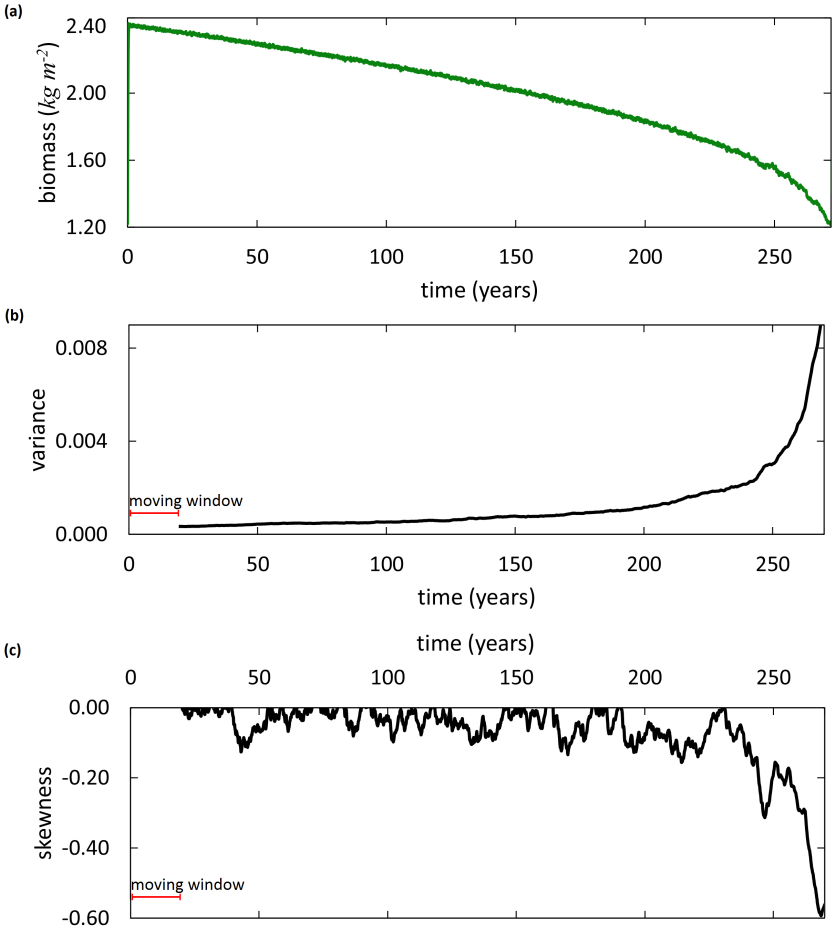

FIGURE 4.12: (a) Time series of biomass. Quantitative measures of variability of the time series: (b) variance and (c) skewness of biomass estimated within moving window of size 10% of the time series.

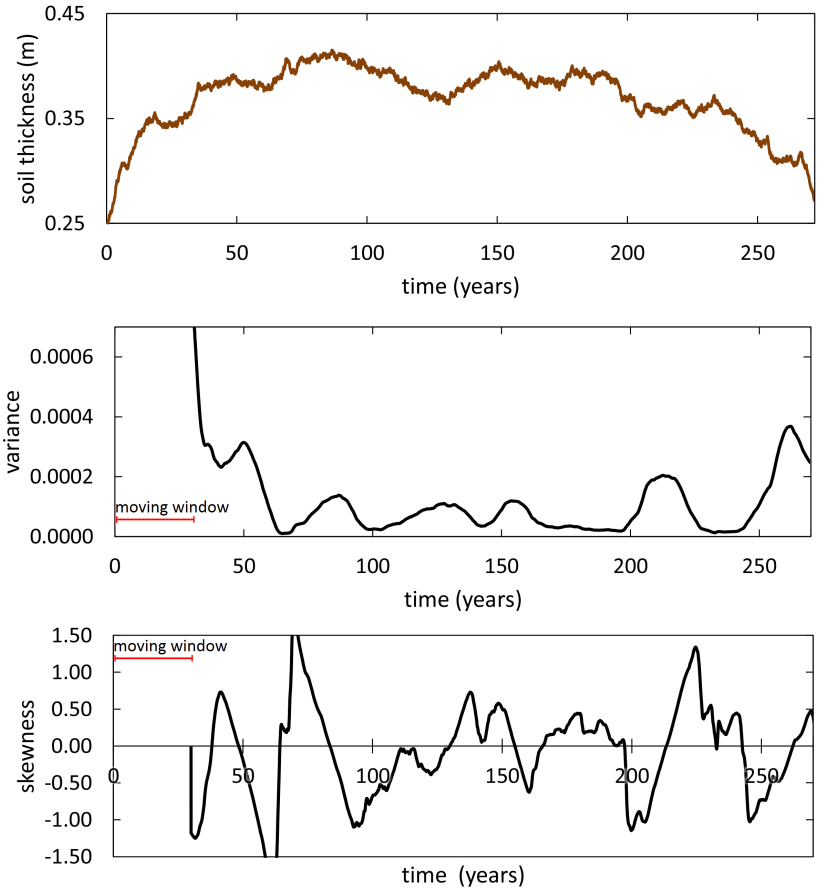

FIGURE 4.13: (a) Time series of soil thickness. Quantitative measures of variability of the time series: (b) variance and (c) skewness of biomass estimated within moving window of size 10% of the time series.

4.4 Multiple realisations and the effect of noise

The stochastic addition utilised in the model leads to the model offering different outputs following each run. The random disturbances cause the critical shift to happen earlier or later. This can be clearly seen from figure 4.14, showing the soil and biomass time series output for 10 model runs (low weathering rate scenario, 4.14a; high weathering rate scenario, 4.14b). At the low bare bedrock weathering rate scenario one observes a distinct difference in the course of collapsing of the system among the transient simulations (around 800y). The same randomness also holds for the high weathering scenario though showing less variability (about 10y). Note that this variability arises from the stochastic disturbances alone.

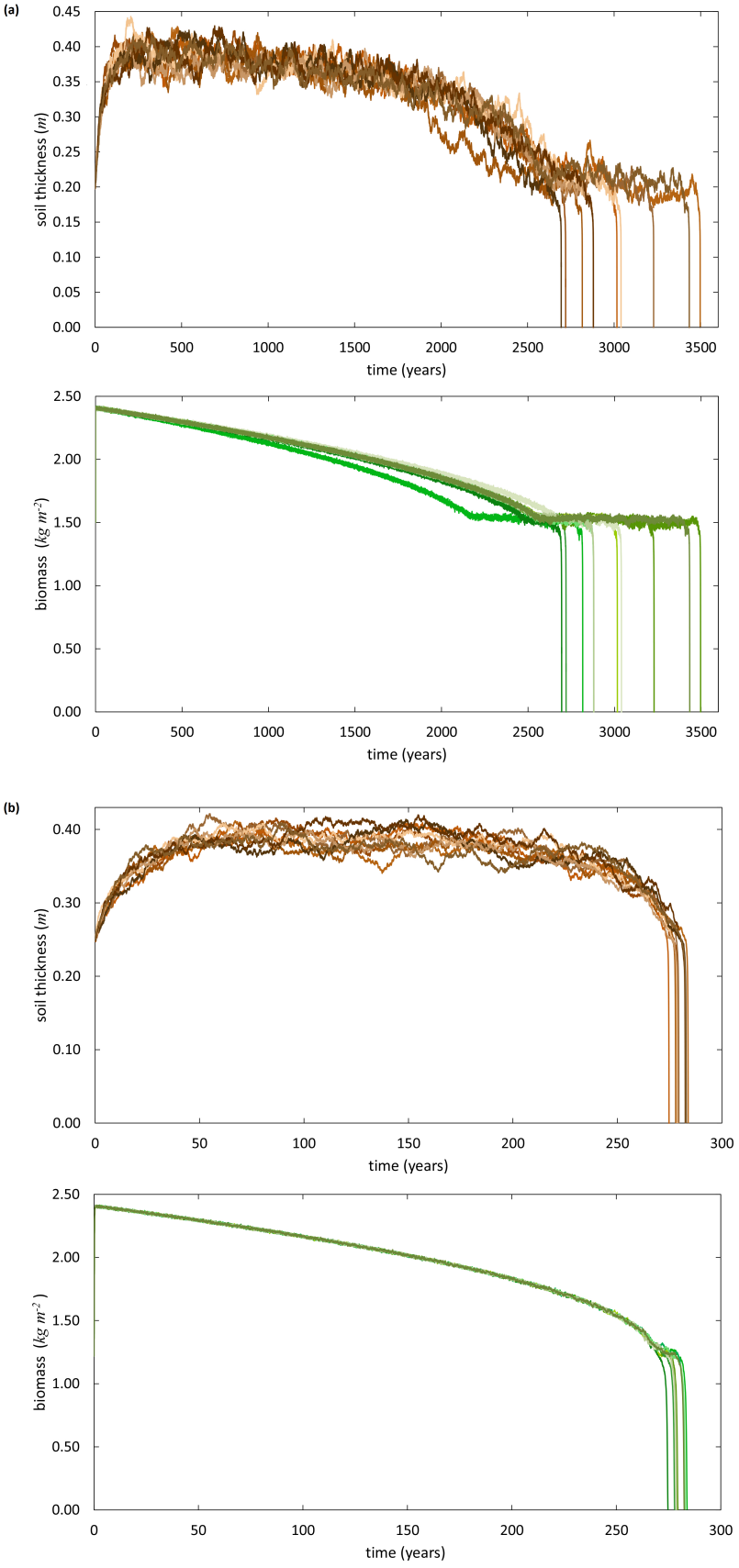

FIGURE 4.14: Soil and biomass time series over 10 simulation runs; (a) low bare bedrock weathering rate scenario and (b) high bare bedrock weathering rate scenario.

Further, of particular importance is the strength of the additive noise. As shown in figure 4.15, increasing the strength of the noise markedly impacts on the duration of the shift– the higher the noise level is, the sooner the system collapses. In particular, at noise level 0.1% the system switches to an unvegetated state within 3800 years. As the magnitude of noise becomes bigger the system will always collapse more quickly (noise level 0.2%, in 3400y; noise level 0.5% in 2500y; noise level 2%, in 1400y) (figure 4.15). This is likely owing to the fact that there may be a larger probability that the system is driven over the edge. The foregoing simulation results correspond to the low bare bedrock weathering rate scenario.

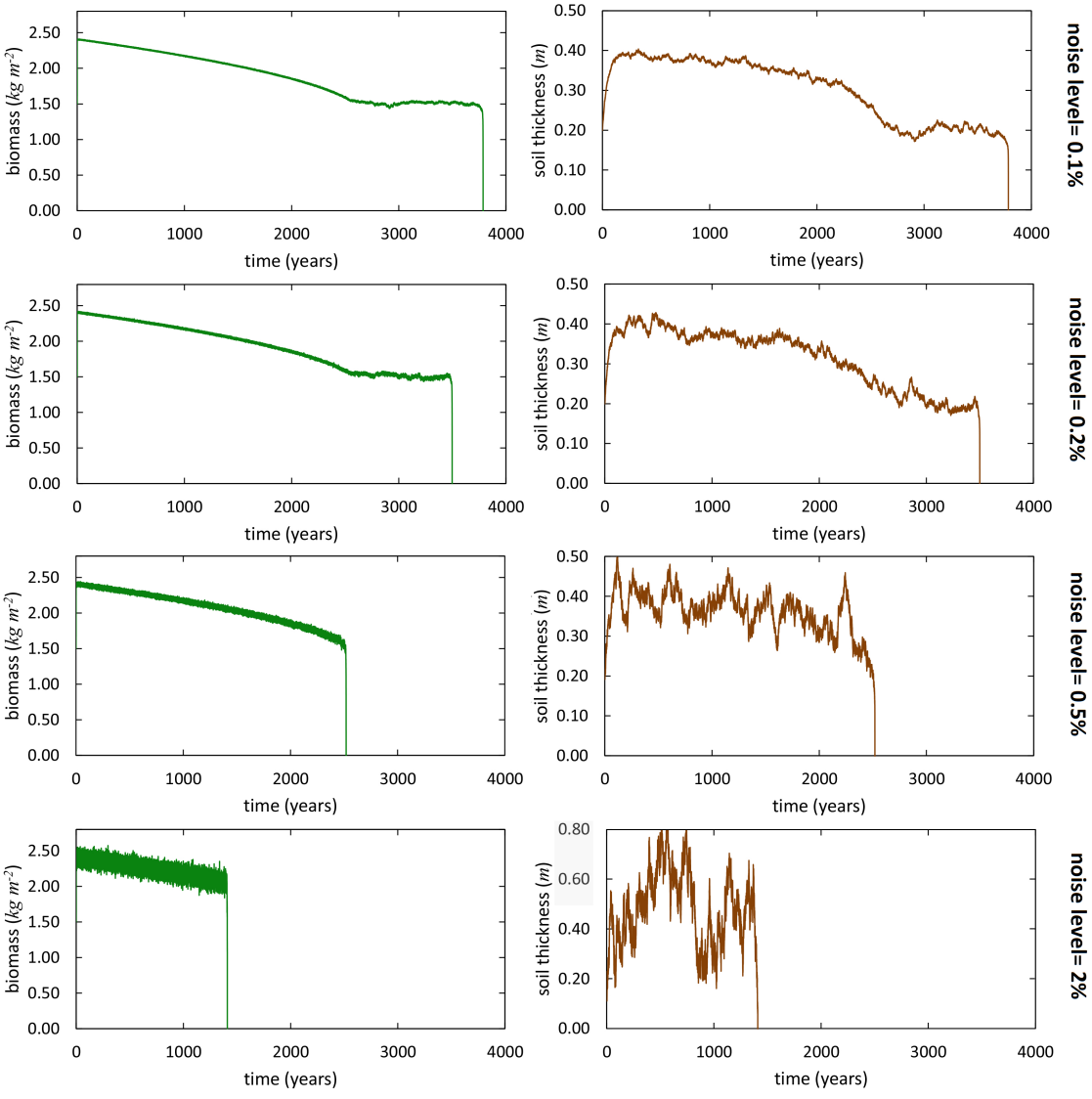

FIGURE 4.15: Biomass and soil thickness model output while increasing the noise level with all the other parameters kept the same (all the plots correspond to the slow transient).

Chapter 5

Discussion

In this study we used a quite straightforward two-dimensional lumped model (Karssenberg, 2014) that represents the basic processes of a semi-arid vegetation-soil system exhibiting a regime shift between alternative stable states under the control of grazing pressure. This is a state transition of a physical system manifesting hysteresis (i.e., the difference in the paths followed by the system during shifting and recovering). Considering that catastrophic regime shifts may happen slowly once going beyond the transition point (Hughes et al., 2013), particular attention was paid to the rate of change throughout the transitional period. We addressed not only how fast the land surface system collapses after a certain point is transgressed, but also applied high-order statistics such as variance and skewness to the simulated time series so as to evaluate their utility as early warning signals. We now move onto discussing our results in the context of the research questions posed in the introductory chapter 1.

5.1 Catastrophic regime shifts may unroll quickly or slowly

The geomorphological system we consider is described by its two constituent subsystems, the soil and the vegetation. It is essentially a mixed system composed of a slow (soil) and a fast (vegetation) components, seeing that the rate of change between these two subsystems is markedly different (Karssenberg, 2014). On inspecting the phase-plane graph, one can observe that the arrows are pointed towards north-south, meaning that the system most rapidly changes along the course of biomass, as the rate of change in biomass is bigger (figure 4.1). That being said, it is not applicable to the points near to the vegetation equilibrium, and nor does at small soil thickness or biomass values.

These speed-wise differing subsystems relate specifically to the manner at which the critical shift unrolls. Our findings showed that there is distinct difference between the two

model scenarios (figure 4.2, 4.3). With one setting (low bare bedrock weathering rates), it is mainly the soil subsystem that reaches the shift. Soil behaves very slowly owing to the low rates of change. Consequently, the system exhibits a progressive transition developing over some hundreds of years. In the other situation (high bare bedrock weathering rates), it is mainly the vegetation subsystem that collapses first, and then the soil collapses. This is done much more quickly, unwinding within a few years.

Ergo, we could say that our land surface system is quite easily affected by adjusting the soil parameters. This greatly influences the response of the system even after passing the point of instability. The foregoing exactly concur with Karssenberg and Bierkens (2014) and Karssenberg (2014).

5.2 Variance and skewness as diagnostic indices of the upcoming shifts

In our analysis, we produced early warning signals based on both variance and skewness exploring two unlike scenarios corresponding to different soil parameters. Generally, we found slightly differing results between these indicators, nevertheless both show peaks prior to the occurrence of the tipping point, fundamental for any early warning signal. It turns out that statistical anomalies appeared in vegetation biomass as manifestations of critical slowing down, whereas no apparent trends found in soil thickness. The latter was likely because the soil subsystem is a pretty slow system. Soil time series exhibit a slower pattern as the variation has a larger range. It therefore seems highly improbable to observe apparent changes in such kinds of system components since one might need much greater time periods to detect possible characteristic trends (e.g. figure *A*.6).

To be more specific, concerning the slowly unfolding critical shift, rising variance in biomass serves as early warning signal prior to the critical point, as does skewness, peaking just ahead of the instability point. On top of that, but less clearly, variance seems to proclaim the true shift (hardly building-up) while skewness does not (figure 4.7). The aforementioned statistical properties of soil thickness seem to fail signalling the catastrophic shift (figure 4.8). Moreover, in the situation of the typical, fast transient response, as expected, the variability visibly increases on the biomass time series, as does the asymmetry in the fluctuations (figure 4.9, 4.11). Our results indicate that variance and skewness of biomass performed well as indicators signalling the upcoming shift (figure 4.12). The foregoing findings are summarised in the table 5.1, simply showing in which occasion indicators announce the approaching shift.

Critical shift	Slowly unfolding regime shift		Quickly unfolding regime shift	
Indicators	Variance	Skewness	Variance	Skewness
Biomass	CriticalPoint$^{\bullet}$ TrueShift$^{\bullet}$	CriticalPoint$^{\bullet}$ TrueShift$^{\circ}$	$\bullet$	$\bullet$
Soil thickness	CriticalPoint$^{\circ}$ TrueShift$^{\circ}$	CriticalPoint$^{\circ}$ TrueShift$^{\circ}$	$\circ$	$\circ$

TABLE 5.1: Early warning signals for low and high bare bedrock weathering model scenarios (black bullets, when the indicator signifies the shift; white bullets, when it fails to announce the shift).

In addition, for fast transient response, besides the increasing variance the actual shift is preceded by a progressive decline in biomass (figure 4.12a). So we could say that both biomass and its variance may be interpreted as indicators. In contrast, when looking at long-lasting transient, biomass itself is barely decreasing prior to the actual switch point – it remains nearly the same between 2600 and 3400y (figure 4.7a). Therefore, in this instance we can solely utilise the early warning signal.

Commenting on the performance of the proposed indicators, we could say that the variance seems to behave slightly finer as early warning over skewness. This is due to the increase in variance occurring several hundred time steps earlier than the peaking seen in skewness (i.e., around 800y at the low bare bedrock weathering rate scenario, figure 4.7; around 50y at the high bare bedrock weathering rate scenario, figure 4.12). Nevertheless there exists one noteworthy issue in the use of variance for an early warning indicator. The rise in variance is gradual towards its peak prior to the critical threshold. This causes a problem in foreseeing the imminence of the critical point itself once an increase in variance is discerned. Skewness on the other hand rapidly diverges from zero to become more negative. This has the advantage that when a notable decline in skewness occurs, the imminence of the critical point is more predictable. In any case, we could say that neither of these is considered to be more effective in treating individually to diagnose the imminence of shift (Guttal and Jayaprakash, 2008; Dakos et al., 2012).

Moreover, for both scenarios we found an increase in variance of biomass before the tipping point ('technically' critical point). Comparing the magnitude of the increasing variance between the gradual transition (increase in variance prior to the critical point) (figure 4.7) and the fast response (increase in variance prior to the critical point– equivalent to the actual shift point) (figure 4.12), we can observe that the degree of growth in variance is almost the same. We could therefore say that the predictability of the 'technically' critical threshold of the system for the fast and the slow transient seems to be more or less identical. Nevertheless, this may not be sufficient in reflecting an upcoming gradual shift corresponding to a slow trajectory of change, since it may be still more protracted after transgressing the critical point and thus perhaps passes unnoticed.

Recapping, our work suggests that the statistical indices of vegetation biomass may exhibit a noticeable change (increasing variance or decreasing skewness) before the tipping point, serving in this way as early warning indicators; nonetheless, they may miss the mark when the system shows long transient behaviour. Importantly, this underscores the sizeable uncertainty over predicting slow catastrophic regime transitions (e.g. Frank et al. (2011); Karssenberg (2014)) ensuing from the prolonged transient phase together with the system dynamics after transcending the critical threshold.

5.2.1 The noise level effect

An interesting observation is that stochastic dynamics of the model play an important role in its behaviour, lead to the model offering different outputs following each run (e.g. figure 4.14). This variability is a result of the stochastic variable per se (no parameters were changed). Although taking a quite low noise level (0.2%), noticeable differences occurred in the course of collapsing of the system, especially for the slow transient scenario (figure 4.14a). In this regard, we chose to analyse a realisation at which the system collapsing very late.

Furthermore, the patterns produced using higher magnitude of noise exhibit shorter collapses (figure 4.15). This is because strong noise levels affect the processes of the model by increasing the probability of the system to be pushed over the limit. This variability may has a significant effect on the duration of the early warning, with some critical points possibly receiving suitable warning, whereas others receiving little or none (e.g. Perretti and Munch (2012)).

5.3 Comparison with other studies, remarks and future directions

Our analysis shows that discernible changes in variance and skewness of biomass perform as indicators of nearness to a certain threshold where the system starts turning to another state, as suggested in the previous studies (e.g. Carpenter and Brock (2006); Guttal and Jayaprakash (2008); Carpenter et al. (2008)). We investigated the use of diagnostic indicators based on biomass and soil, nonetheless the results presented here, provide strong support for the use of these early warning signals across a multitude of disciplines including climate, biology and finance. Notwithstanding differences, one may successfully apply these indicators in any system with a tipping point, based on its universal properties; and this gives special value to their potential for forewarning, albeit the restricted knowledge of the underlying behaviour of the system.

In addition to time series data, spatial patterns could be analysed providing value-added indicators, insofar as they can support additional information compared to a single point in time (Scheffer et al., 2012). To this effect, it would be an interesting extension to treat spatial indicators by utilising the fully-distributed process-based model. The combination of both temporal and spatial indicators perhaps improves the dependability of the signals (Dakos et al., 2012). In this regard, further work into the full spatial system so as to build composite indicators is desirable.

It is important to note that despite the encouraging fact that some few recent studies have dealt with the detection of early warnings in real data (e.g. Dakos et al. (2008); Drake and Griffen (2010); Carpenter and Brock (2011); Dai et al. (2013)), it is still highly challenging to use this in reality. To this effect, possible flaws can be found in view of the requirement of large volumes of high resolution data (Dakos et al., 2008; Karssenberg and Bierkens, 2012), lacking understanding of indicators' behaviour in considerably complex systems (Scheffer et al., 2012) and the ineffectiveness of administrative policy processes (Biggs et al., 2009).

Therefore the question remains concerning the applicability of these findings to real world scenarios. For instance, the utilisation of either of these early warning signals described above requires the continued measurement of biomass and soil through time in order for the variance and skewness to be calculated and monitored for changes. Also, a further shortcoming emerges with regard to averting critical transitions is that the parameter values, and the relationships between them, that the model uses to determine the usefulness of the early warning indicators will surely vary depending on vegetation type, soil type and climate.

On conditions that the threshold responses become slow, the likelihood of forestalling them considerably reduces or even nullifies. It is of the essence here to emphasise the increased risk of false warnings or ambiguous signals (e.g. Dakos et al. (2012); Guttal et al. (2013); Dakos et al. (2015)) for the slow transients. Hence, the discrimination between rapid and slow transitions looks to be critically important (Hughes et al., 2013). With this in mind, we should further research into elucidating such long-lasting transients and yet more into evaluating the robustness of the postulated early indicators in slow responding systems. Moreover, regarding the applicability of our findings in reality, an important direction of future work should involve empirical tests on field observations. One for example would focus on developing statistical methods to investigate the phenomenon of time-delays in consequence of producing slow, transient responses in real data, as suggested by Guttal et al. (2013).

Recalling that the spatially-lumped model used here is derived from a high-resolution model which describes the ecohydrological processes of a land surface system incorporating spatially varying data. In this regard, we would like to underline the strength of this approach as suggested by Karssenberg (2014), in view of the successful combination of the two models. The distributed model gives a more circumstantial representation of the geomorphological system while the low resolution model allows deriving analytical approximations. Despite of being minimalistic, it represents well the fundamental processes of the vegetation-soil system. Additionally, the lumped simulation offers fast computation time. Consequently, one may equally apply this novel approach to a multiplicity of other systems consisting of many coupled units in order to develop a better understanding of their functioning (Karssenberg, 2014).

Despite the possible pitfalls involved, coming up with statistical procedures that provide evidence for the imminence of the system to upcoming regime shifts is absolutely valuable. Considering their capacity for practical application though, conditions are rather far from ideal especially to ecological systems that may exhibit long transient phases. In order to make the early warning signals more functional in predicting unwanted changes we have to tackle the underlying deep uncertainty. To this end, the development of integrating modelling, monitoring and management approaches is still required.

Chapter 6

Conclusions

In this research project we studied a semi-arid land surface system which undergoes a critical transition between two contrasting states associated to hysteresis. For this, we employed a two-dimensional, spatially-lumped model (Karssenberg, 2014) that simulates the fundamental processes of a soil-vegetation system by testing it under two differing soil parameter settings. At the same time, we investigated the usage of variance and skewness of biomass and soil time series data as early warning indicators for such catastrophic changes.

It turns out that when the system crosses the switch point, the unwanted shift occurs either classically fast, having a transitional period just about a few years, or unexpectedly slow unfolding over hundreds or even thousands of years. This considerable difference in transient dynamics ensues from altering bare bedrock weathering rates. Our analysis also suggests that the variance and the skewness of vegetation biomass may serve as early warning signals of the forthcoming critical shift, whereas statistic signatures of soil thickness does not provide clear trends. Importantly, in case the transitional period lasts longer (i.e., the regime shift unfolding very slowly), the actual switch is somehow problematic to detect. In particular, although the proposed indicators show characteristic trends prior to the 'technically' critical point, they may be lacking power to detect the true collapse. Notwithstanding forewarnings of the critical point, it is distinctly possible that a systemic transition may pass unnoticed. This spotlights the great uncertainty when it comes to predicting the timing of the shift.

Though the assorted constraints, early warning signals of critical transitions certainly provide important clues in the dynamics of the system which further our ability to forecast radical systemic changes. This is mainly based on their certain generic character (Scheffer et al., 2009), nonetheless the task of their practical application is still

challenging (Dakos et al., 2015). Working towards bettering the power of early warning indicators, further research should concentrate on the better understanding of the dynamics and critical changes in systems with smooth and slow threshold responses. Additionally, complementing multifarious indicators (temporal and spatial) could be an important direction of future work since it is considered rather promising in the prognosis of an undesirable collapse (e.g. Carpenter et al. (2011); Dakos et al. (2011)). Lastly, given that the applicability of these findings to real world scenarios remains an open question, field testing will be needed to verify the reliability of the proposed statistical methods in reality.

Appendix A

Supplementary figures

Supplementary figures associated with this study can be found here.

Unfolding of critical transition

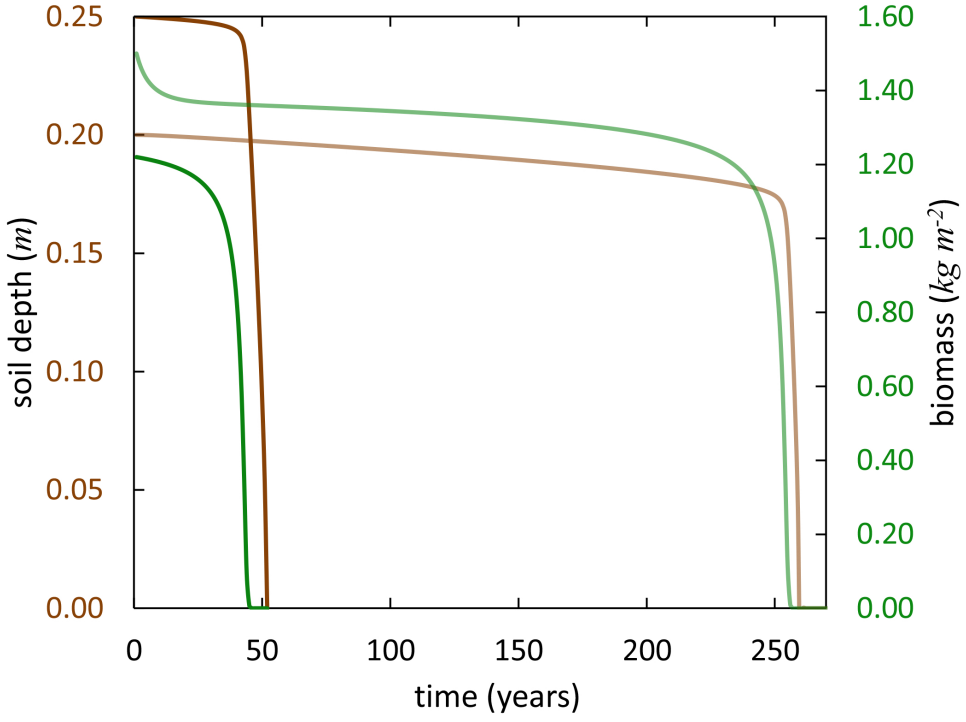

FIGURE A.1: The transient response between the two alternative stable states for the low bare bedrock weathering scenario (pale colored lines) and for the high bare bedrock weathering scenario (deep colored lines) (green lines, biomass; brown lines, soil thickness).

Low bare bedrock weathering scenario (W_0=0.0004, a=3.47)

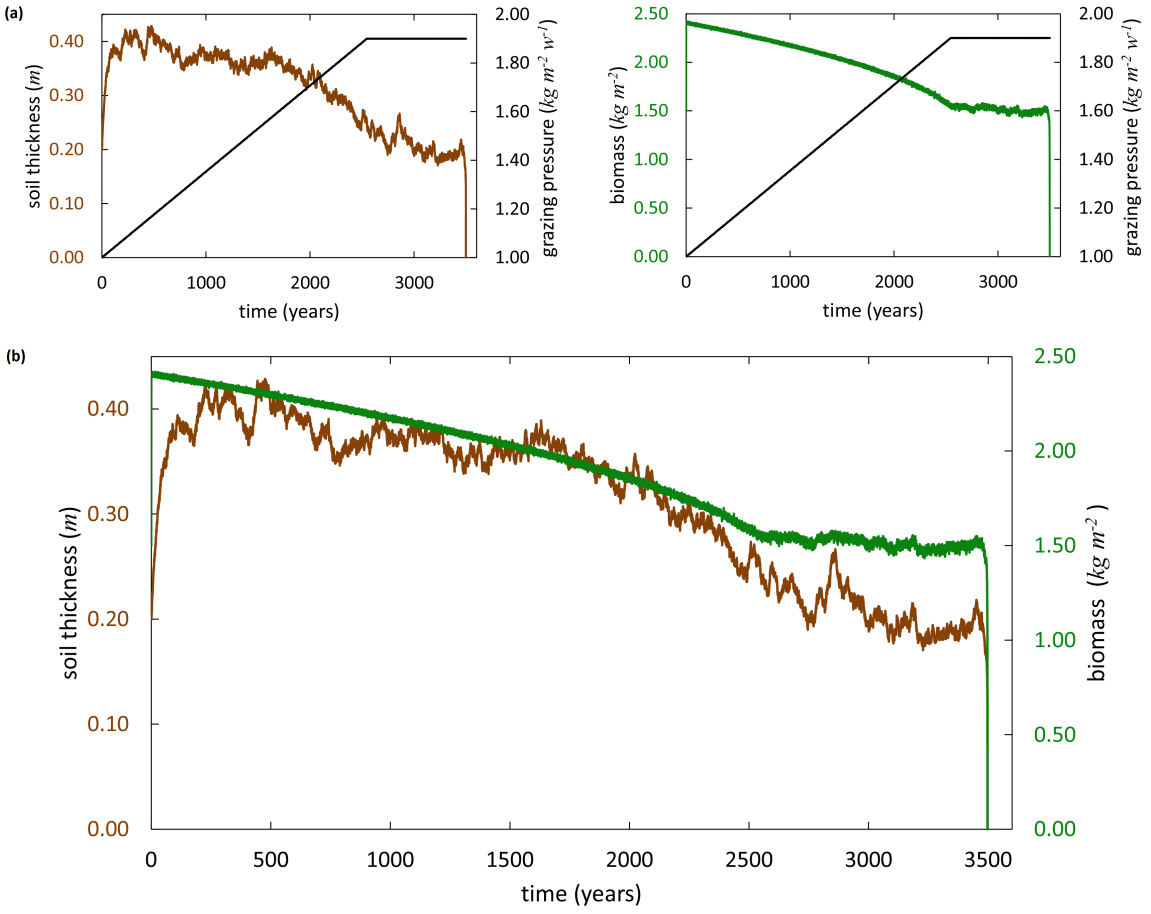

FIGURE A.2: Slowly unfolding regime shift. At the top, time series of biomass (green line; right) and soil thickness (brown line; left) plotted together with grazing rate (black line) against time. At the bottom, combined plot: time series of biomass (green line) and soil thickness (brown line).

High bare bedrock weathering scenario (W_0=0.002, a=7.49)

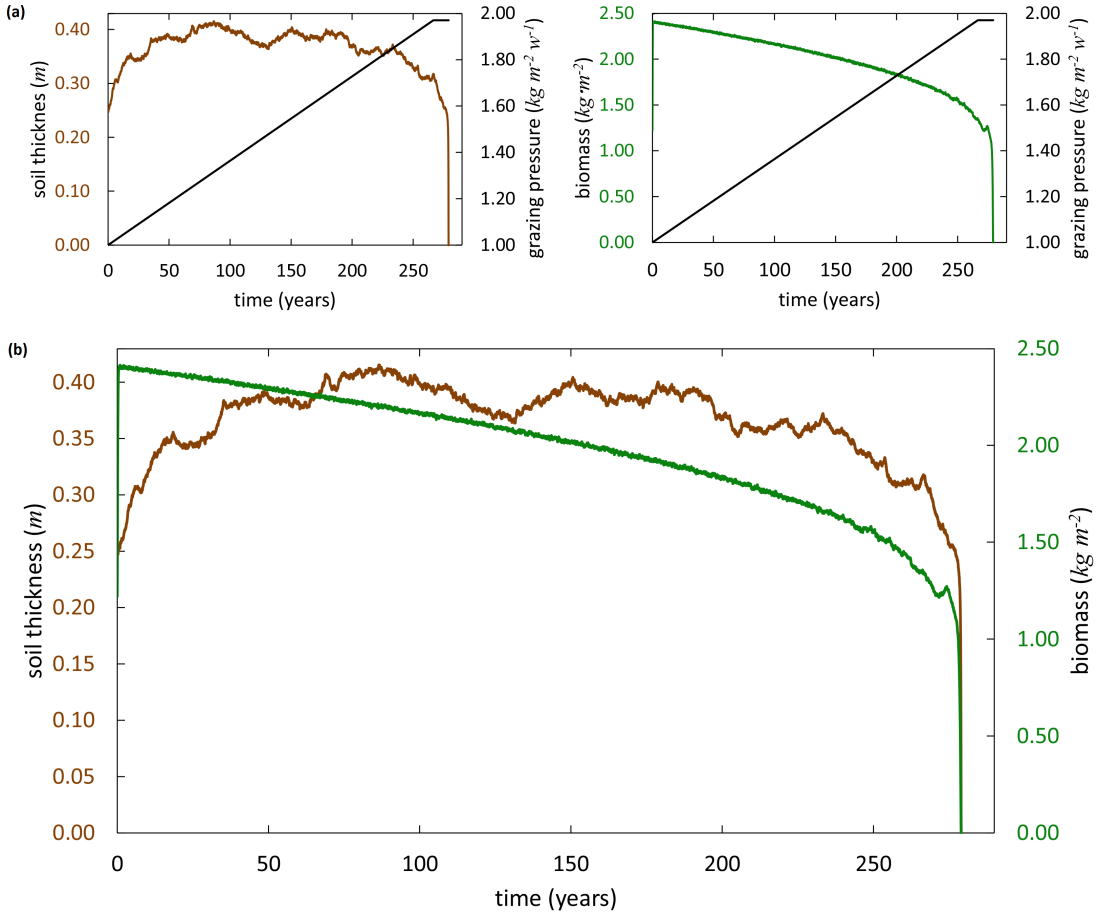

FIGURE A.3: Quickly unfolding regime shift. At the top, time series of biomass (green line; right) and soil thickness (brown line; left) plotted together with grazing rate (black line) against time. At the bottom, combined plot: time series of biomass (green line) and soil thickness (brown line).

Multiple realisations

High bare bedrock weathering rate scenario

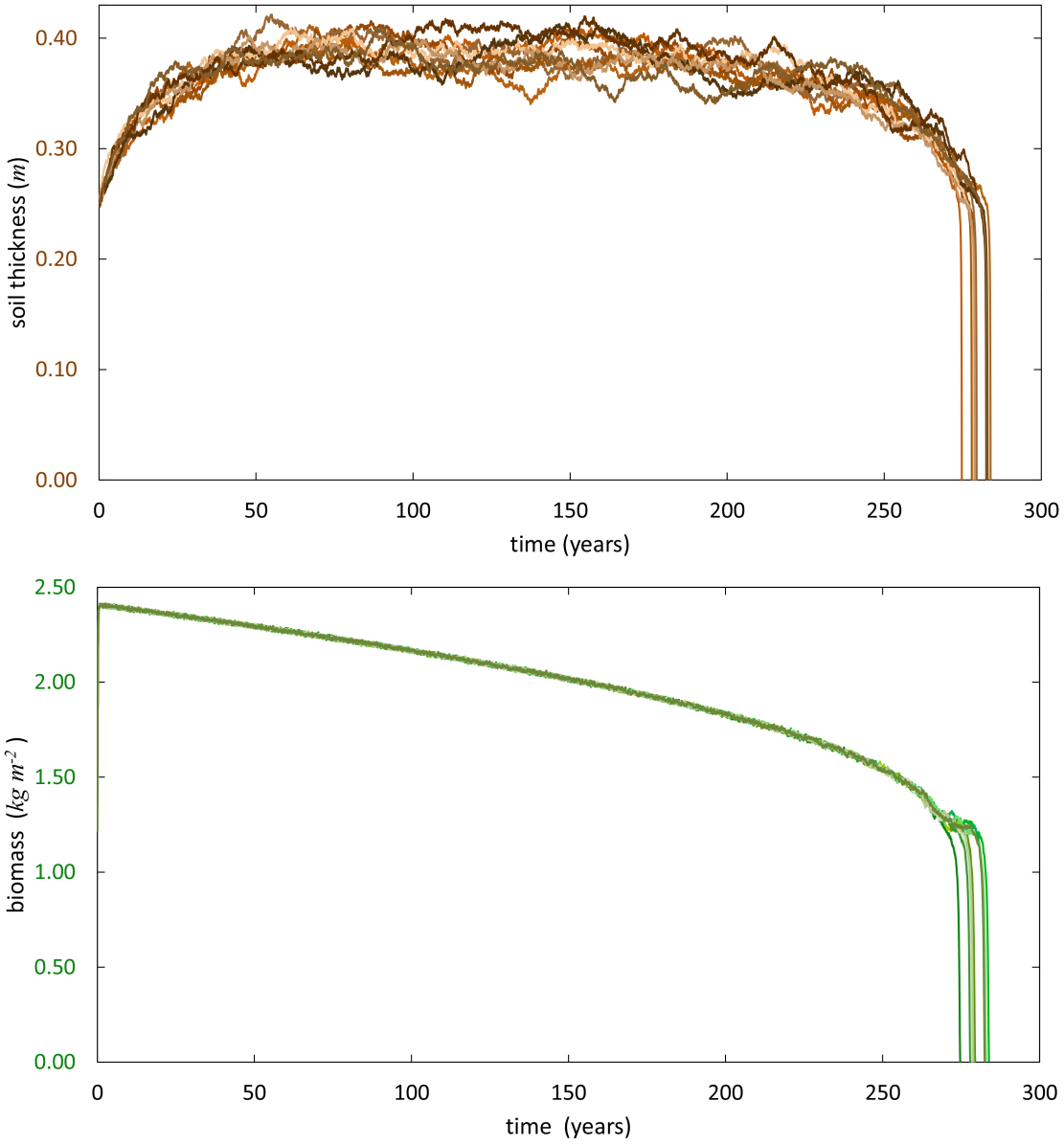

FIGURE A.4: Soil and biomass time series output for 10 runs. Each individual line shows one model run.

Low bare bedrock weathering rate scenario

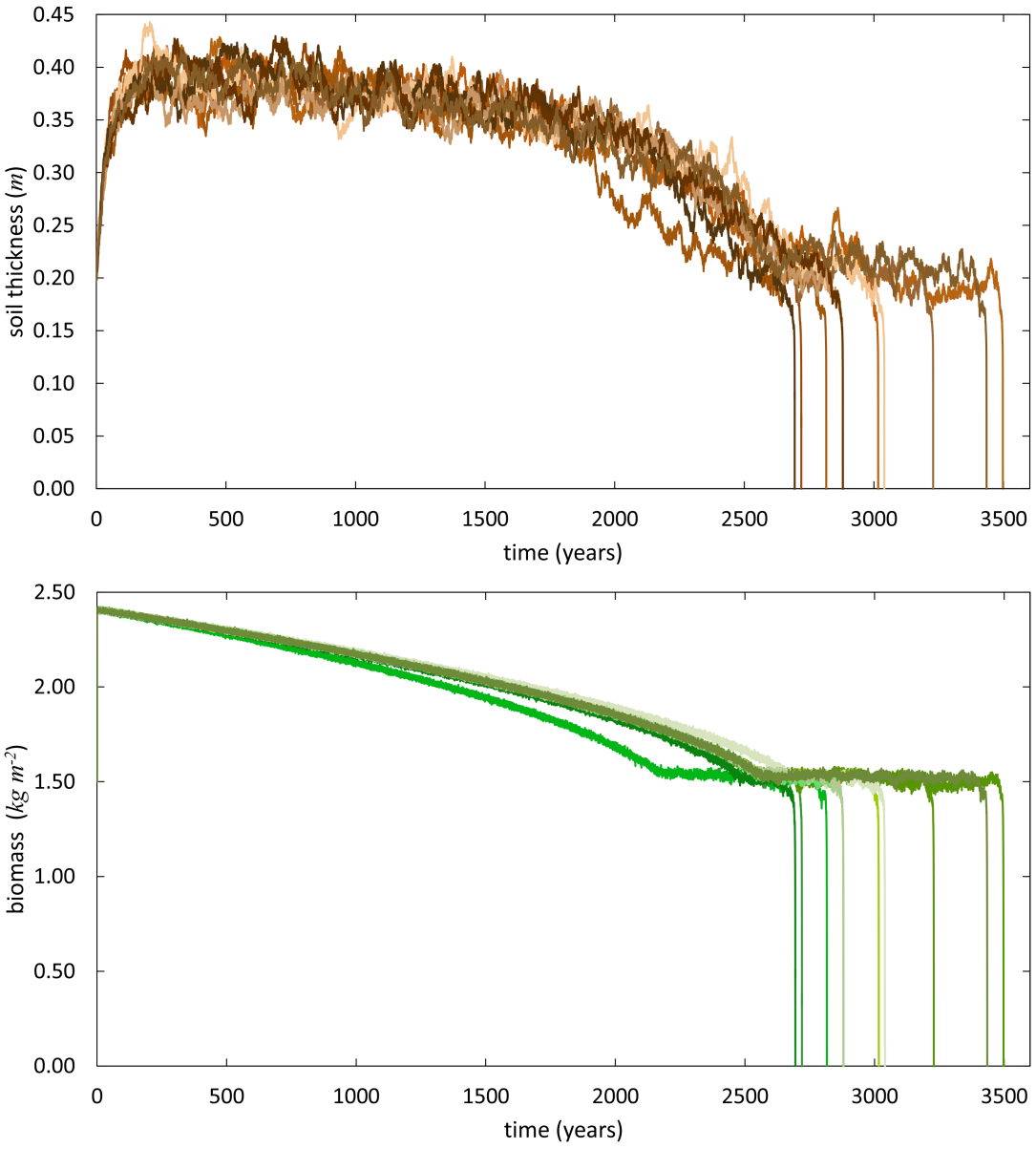

FIGURE A.5: Soil and biomass time series output for 10 runs. Each individual line shows one model run.

Test run

Longer runtime

Here we consider an even longer run representing a hypothetical situation where one would have a really slow system. We take a realisation of 936000 time steps by increasing the grazing pressure by only $1 \cdot 10^{-6}$ units each time step, so as to get rid of the observed variation. Interestingly, it can be showed that the trend tends to be slightly smoothed out and the estimated variance reveals a characteristic pattern (this run corresponds to the low bare bedrock weathering rate scenario).

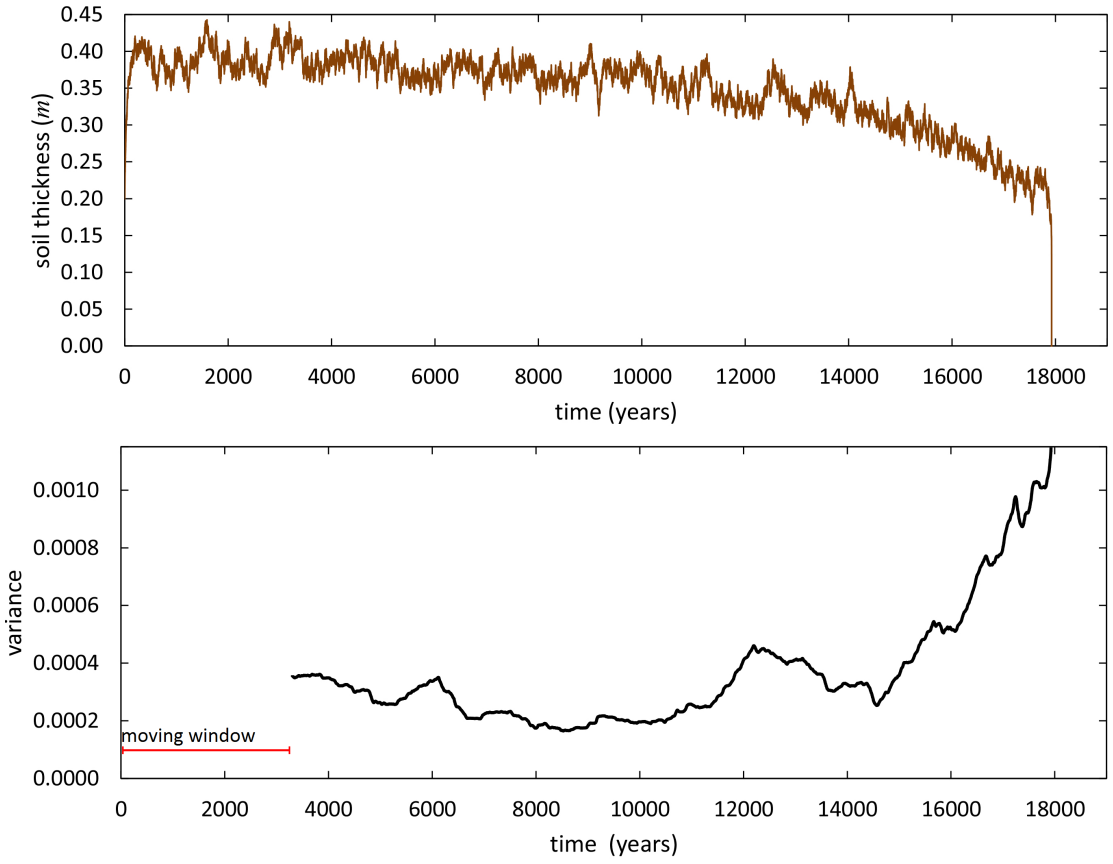

FIGURE A.6: Top, soil time series output for a very long runtime (i.e., 936000 time steps); below, variance estimated within moving window of 18% the size of the time series.

Appendix B

Mathematical operations

Estimating the steady-state solution

We find the equilibria for the soil and the vegetation subsystems by setting the rate of change equal to 0 and solving the resulting algebraic equations. This is done as follows:

$$\frac{dD}{dt} = W_0 e^{-aD} - e^{-B/b}(E_t + e^{-D/c}(E_0 - E_t)) - C \tag{B.1}$$

$$\frac{dD}{dt} = f(D) = 0$$

$$-e^{-B/b} = \frac{e - W_0 e^{-aD}}{(E_t + e^{-D/c}(E_0 - E_t))}$$

$$e^{-B/b} = \frac{W_0 e^{-aD} - C}{E_t + e^{-D/c}(E_0 - E_t)}$$

$$-\frac{B}{b} = ln\left(\frac{W_0 e^{-aD} - C}{E_t + e^{-D/c}(E_0 - E_t)}\right)$$

$$B = -b \cdot ln\left(\frac{W_0 e^{-aD} - C}{e^{-D/c}(E_o - E_t) + E_t}\right)$$

$$
\begin{aligned}
\frac{dB}{dt} = (1-(1-i)e^{-D/d})\left(rB\left(1-\frac{B}{c}\right)\right) - g\left(\frac{B}{s+B}\right) \\
\frac{dB}{dt} = f(B) = 0 \\
\left(1-(1-i)e^{-\frac{D}{d}}\right)\left(rB(1-\frac{B}{c})\right) = g\left(\frac{B}{s+B}\right) \\
\left(1-(1-i)e^{-\frac{D}{d}}\right) = \frac{g(\frac{B}{s+B})}{rB(1-\frac{B}{c})} \\
\left(1-(1-i)e^{-\frac{D}{d}}\right) = \frac{g}{r(s+B)(1-\frac{B}{c})} \\
-(1-i)e^{-\frac{D}{d}} = \frac{g}{r(s+B)(1-\frac{B}{c})} - 1 \\
i \cdot e^{-\frac{D}{d}} = \frac{g}{r(B+s)(1-\frac{B}{c})} \\
D = -d \cdot ln\left[\frac{g}{i \cdot r(B+s)(1-\frac{B}{c})}\right]
\end{aligned}
\tag{B.2}
$$

Appendix C

Programming Information

This provides a concise summary relating to the programming part. Note that the process-based distributed model was built within PCRaster Python framework (for full details refer to Karssenberg et al. (2015)). The lumped model is formed by two differential equations (3.1 & 3.2), essentially capturing the interaction between the soil and the vegetation systems. Statistical analyses made in PYTHON v.2.7.6 (`https://www.python.org/`) with **pandas** DataFrame. The high-order statistics of the time series data estimated using the `rolling_var` and `rolling_skew` rolling statistics functions. Figures produced using **matplotlib** plotting library.

Below we provide the main script (basic code for the simulations) of the lumped model, followed by the `simpleParameters.py` function containing the parameters used, `var.py` and `skew.py` functions for calculating mathematical statistics (variance and skewness respectively).

Model scripts

```
# main simulation script

import math
import generalfunctions
from pcraster import *
from pcraster.framework import *
from simpleModelFunctions import *
from simpleParameters import *

# time step is a week
nrOfSamples = 1
numberOfTimeSteps=52 * 1000

multiplierDeposition=1.0

findEquilibrium=False
passWeatheringParameters=False

class CatchmentModel(DynamicModel,MonteCarloModel):
  def __init__(self):
    DynamicModel.__init__(self)
    MonteCarloModel.__init__(self)
    setclone('clone.map')
    setrandomseed(101)

  def premcloop(self):
    print 'done'

  def initial(self):
    # timestep duration in hours
    self.timeStepDuration = 7.0 * 24.0

    # normal execution: take all from simpleParameters.py
    self.weatheringRateBareBedrock=weatheringRateBareBedrock
    self.weatheringExponentParameter=weatheringExponentParameter

    self.slope=1.00 # low scen.,1.9390; high scen.,1.9660
    self.thickness=0.20 # low scen.,0.20; high scen.,0.25
    self.biomass=1.50 # low scen.,1.50 ;high scen.,1.22

    self.thickLi=[]
    self.bioLi=[]
    self.slopeLi=[]

    self.durationToDegraded=-9999.0
    self.durationToDegradedStored=False

  def dynamic(self):
    if self.currentTimeStep() % 1 == 0 or (self.currentTimeStep() == 1):
      self.thickLi.append(self.thickness)
      self.bioLi.append(self.biomass)
      self.slopeLi.append(self.slope)
```

```
    bioGrowth=growth(self.biomass,self.thickness,carryingCapacity, \
              growthRateParameter,regolithRange, regolithIntercept)
    bioGrazing=grazing(self.biomass, intercept, self.slope)

    self.biomass=self.biomass+self.timeStepDuration*((bioGrowth-bioGrazing)\
                 /(52.0*24.0))
    # add noise; low scen., 0.003; high scen., 0.00244
    self.biomass=self.biomass+np.random.normal(0, 0.003)

    # increase the grazing pressure
    if self.slope<1.9000:
        self.slope= self.slope + 0.00000100 # low scen., 6.8*10e-6; high scen., 7*10e-5
    else:
        self.slope= self.slope + 0

    regWeathering=weathering(self.thickness,self.weatheringRateBareBedrock, \
                  self.weatheringExponentParameter)
    regErosion=erosion(self.thickness,self.biomass,erosionRateBareBedrockThickZero, \
               erosionRateBareBedrockThickMax, \
               erosionExponentParameter,vegetationRange)

    self.thickness=self.thickness+multiplierDeposition*(regWeathering-regErosion)/1.0

    # add noise; low scen., 0.0004; high scen., 0.0005
    self.thickness=self.thickness+np.random.normal(0, 0.0004)

    if self.thickness < 0.01 and not self.durationToDegradedStored:
      self.durationToDegraded=self.currentTimeStep()
      self.durationToDegradedStored=True

    if self.currentTimeStep() == numberOfTimeSteps:
      numpy.save('thick.npy',self.thickLi)
      numpy.save('bio.npy',self.bioLi)
      numpy.save('slope.npy',self.slopeLi)
      numpy.save('durationToDegraded.npy',self.durationToDegraded)

  def postmcloop(self):
    print 'done'

myModel = CatchmentModel()
dynamicModel = DynamicFramework(myModel, numberOfTimeSteps)
mcModel = MonteCarloFramework(dynamicModel, nrOfSamples)
mcModel.setForkSamples(True,2)
mcModel.run()
```

```
# simpleParameters (the parameters used in the model)

# low scenario
weatheringRateBareBedrock=0.0004
weatheringExponentParameter=3.47

# high scenario
weatheringRateBareBedrock=0.002
weatheringExponentParameter=7.49

vegetationRange = 0.28
meanErosionRate=0.0008*52.0
factor=2.01
erosionRateBareBedrockThickMax = meanErosionRate/factor
erosionRateBareBedrockThickZero = meanErosionRate*factor
erosionExponentParameter= 20.0
growthRateParameter=2.1
carryingCapacity=2.9
regolithRange=0.04
regolithIntercept=-0.7
intercept=0.2

# grazing pressure
slope=1.00 # low scen., 1.9390; high scen., 1.9660
```

```
# calculate rolling variance

import pandas as pd
import numpy as np

#data = numpy.loadtxt('biomass.txt')
#bio_data=data
bio_data=bio
# type(bio_data)

inda=np.arange(1,181876)
df = pd.DataFrame(bio_data[:], index=inda[:])

# plot the time series
df.plot(style='k--')

# calculate the rolling mean and plot
pd.rolling_mean(ts,2600).plot(style='k')

# add the rolling variance:
pd.rolling_var(df,2600).plot(style='b')

var=pd.rolling_var(df,2600)
np.savetxt('var_biomass.txt', var, fmt='%.10f', newline=os.linesep)
```

```
# calculate rolling skewness

import pandas as pd
import numpy as np

#data = numpy.loadtxt('biomass.txt')
#bio_data=data
bio_data=bio
# type(bio_data)

inda=np.arange(1,181876)
df = pd.DataFrame(bio_data[:], index=inda[:])

# plot the time series
df.plot(style='k--')

# calculate the rolling mean and plot
pd.rolling_mean(ts,5200).plot(style='k')

# add the rolling skewness:
pd.rolling_skew(df,5200).plot(style='b')

skew=pd.rolling_skew(df,5200)
np.savetxt('skew_biomass.txt', skew, fmt='%.10f', newline=os.linesep)
```

Bibliography

M. R. Aguiar and O. E. Sala. Patch structure, dynamics and implications for the functioning of arid ecosystems. *Trends in Ecology & Evolution*, 14(7):273–277, 1999.

C. L. Alados, A. ElAich, V. P. Papanastasis, H. Ozbek, T. Navarro, H. Freitas, M. Vrahnakis, D. Larrosi, and B. Cabezudo. Change in plant spatial patterns and diversity along the successional gradient of mediterranean grazing ecosystems. *Ecological Modelling*, 180(4):523–535, 2004.

J. M. Anderies, M. A. Janssen, and B. H. Walker. Grazing management, resilience, and the dynamics of a fire-driven rangeland system. *Ecosystems*, 5(1):23–44, 2002.

N. Barbier, P. Couteron, J. Lejoly, V. Deblauwe, and O. Lejeune. Self-organized vegetation patterning as a fingerprint of climate and human impact on ssemi-arid ecosystems. *Journal of Ecology*, 94(3):537–547, 2006.

B. E. Beisner, D. T. Haydon, and K. Cuddington. Alternative stable states in ecology. *Frontiers in Ecology and the Environment*, 1(7):376–382, 2003.

E. Benincà. *Is there chaos out there?: analysis of complex dynamics in plankton communities.* publisher not identified, 2010.

E. Benincà, J. Huisman, R. Heerkloss, K. D. Jöhnk, P. Branco, E. H. Van Nes, M. Scheffer, and S. P. Ellner. Chaos in a long-term experiment with a plankton community. *Nature*, 451(7180):822–825, 2008.

G. Bergkamp, A. Cerda, and A. Imeson. Magnitude-frequency analysis of water redistribution along a climate gradient in spain. *Catena*, 37(1):129–146, 1999.

B. T. Bestelmeyer. Threshold concepts and their use in rangeland management and restoration: the good, the bad, and the insidious. *Restoration Ecology*, 14(3):325–329, 2006.

R. Biggs, S. R. Carpenter, and W. A. Brock. Turning back from the brink: detecting an impending regime shift in time to avert it. *Proceedings of the National academy of Sciences*, 106(3):826–831, 2009.

A. J. Bisigato and M. B. Bertiller. Grazing effects on patchy dryland vegetation in northern patagonia. *Journal of Arid Environments*, 36(4):639–653, 1997.

I. Blindow, G. Andersson, A. Hargeby, and S. Johansson. Long-term pattern of alternative stable states in two shallow eutrophic lakes. *Freshwater Biology*, 30(1):159–167, 1993. ISSN 1365-2427. doi: 10.1111/j.1365-2427.1993.tb00796.x.

M. Boer and J. Puigdefábregas. Effects of spatially structured vegetation patterns on hillslope erosion in a semiarid mediterranean environment: a simulation study. *Earth Surface Processes and Landforms*, 30(2):149–167, 2005.

F. Borgogno, P. D'Odorico, F. Laio, and L. Ridolfi. Mathematical models of vegetation pattern formation in ecohydrology. *Reviews of Geophysics*, 47(1), 2009.

W. A. Brock and S. R. Carpenter. Variance as a leading indicator of regime shift in ecosystem services. *Ecology & Society*, 11(2), 2006.

J. H. Brown, T. J. Valone, and C. G. Curtin. Reorganization of an arid ecosystem in response to recent climate change. *Proceedings of the National Academy of Sciences*, 94(18):9729–9733, 1997.

S. Carpenter and W. Brock. Rising variance: a leading indicator of ecological transition. *Ecology letters*, 9(3):311–318, 2006.

S. Carpenter and W. Brock. Early warnings of regime shifts in spatial dynamics using the discrete fourier transform. *Ecosphere*, 1(5):art10, 2010.

S. Carpenter and W. Brock. Early warnings of unknown nonlinear shifts: a nonparametric approach. *Ecology*, 92(12):2196–2201, 2011.

S. Carpenter, W. Brock, J. Cole, J. Kitchell, and M. Pace. Leading indicators of trophic cascades. *Ecology Letters*, 11(2):128–138, 2008.

S. Carpenter, J. Cole, M. Pace, R. Batt, W. Brock, T. Cline, J. Coloso, J. Hodgson, J. Kitchell, D. Seekell, et al. Early warnings of regime shifts: a whole-ecosystem experiment. *Science*, 332(6033):1079–1082, 2011.

S. R. Carpenter. Regime shifts in lake ecosystems: Pattern and variation. *Excellence in Ecology*, 20, 2003.

S. R. Carpenter. Eutrophication of aquatic ecosystems: bistability and soil phosphorus. *Proceedings of the National Academy of Sciences of the United States of America*, 102 (29):10002–10005, 2005.

S. R. Carpenter, D. Ludwig, and W. A. Brock. Management of eutrophication for lakes subject to potentially irreversible change. *Ecological applications*, 9(3):751–771, 1999.

K. K. Caylor, G. S. Okin, L. Turnbull, J. Wainwright, T. Wiegand, T. E. Franz, and A. J. Parsons. Integrating short-and long-range processes into models: The emergence of pattern. In *Patterns of Land Degradation in Drylands*, pages 141–167. Springer, 2014.

J. S. Clark, S. R. Carpenter, M. Barber, S. Collins, A. Dobson, J. A. Foley, D. M. Lodge, M. Pascual, R. Pielke Jr, W. Pizer, et al. Ecological forecasts: an emerging imperative. *Science*, 293(5530):657–660, 2001.

L. Dai, K. S. Korolev, and J. Gore. Slower recovery in space before collapse of connected populations. *Nature*, 496(7445):355–358, 2013.

V. Dakos. *Expecting the unexpected: indicators of resilience as early-warning signals for critical transitions*. Wageningen University, 2011.

V. Dakos, M. Scheffer, E. H. van Nes, V. Brovkin, V. Petoukhov, and H. Held. Slowing down as an early warning signal for abrupt climate change. *Proceedings of the National Academy of Sciences*, 105(38):14308–14312, 2008.

V. Dakos, E. H. van Nes, R. Donangelo, H. Fort, and M. Scheffer. Spatial correlation as leading indicator of catastrophic shifts. *Theoretical Ecology*, 3(3):163–174, 2010.

V. Dakos, S. Kéfi, M. Rietkerk, E. H. van Nes, and M. Scheffer. Slowing down in spatially patterned ecosystems at the brink of collapse. *The American Naturalist*, 177 (6):E153–E166, 2011.

V. Dakos, S. R. Carpenter, W. A. Brock, A. M. Ellison, V. Guttal, A. R. Ives, S. Kefi, V. Livina, D. A. Seekell, E. H. van Nes, et al. Methods for detecting early warnings of critical transitions in time series illustrated using simulated ecological data. *PloS one*, 7(7):e41010, 2012.

V. Dakos, E. H. van Nes, and M. Scheffer. Flickering as an early warning signal. *Theoretical Ecology*, 6(3):309–317, 2013.

V. Dakos, S. R. Carpenter, E. H. van Nes, and M. Scheffer. Resilience indicators: prospects and limitations for early warnings of regime shifts. *Philosophical Transactions of the Royal Society B: Biological Sciences*, 370(1659):20130263, 2015.

G. M. Daskalov, A. N. Grishin, S. Rodionov, and V. Mihneva. Trophic cascades triggered by overfishing reveal possible mechanisms of ecosystem regime shifts. *Proceedings of the National Academy of Sciences*, 104(25):10518–10523, 2007.

A. M. de Roos and L. Persson. Size-dependent life-history traits promote catastrophic collapses of top predators. *Proceedings of the National Academy of Sciences*, 99(20): 12907–12912, 2002.

P. D'Odorico and A. Porporato. Preferential states in soil moisture and climate dynamics. *Proceedings of the National Academy of Sciences of the United States of America*, 101(24):8848–8851, 2004.

R. Donangelo, H. Fort, V. Dakos, M. Scheffer, and E. H. Van Nes. Early warnings for catastrophic shifts in ecosystems: comparison between spatial and temporal indicators. *International Journal of Bifurcation and Chaos*, 20(02):315–321, 2010.

T. J. Done. Phase shifts in coral reef communities and their ecological significance. In *The Ecology of Mangrove and Related Ecosystems*, pages 121–132. Springer, 1992.

J. M. Drake and B. D. Griffen. Early warning signals of extinction in deteriorating environments. *Nature*, 467(7314):456–459, 2010.

H. T. Dublin, A. Sinclair, and J. McGlade. Elephants and fire as causes of multiple stable states in the serengeti-mara woodlands. *Journal of Animal Ecology*, 59(3):1147–1164, 1990.

D. Dunkerley and K. Brown. Oblique vegetation banding in the australian arid zone: implications for theories of pattern evolution and maintenance. *Journal of Arid Environments*, 51(2):163–181, 2002.

J. A. Estes and D. O. Duggins. Sea otters and kelp forests in alaska: generality and variation in a community ecological paradigm. *Ecological Monographs*, 65(1):75–100, 1995.

C. P. Fernandez-Illescas and I. Rodriguez-Iturbe. The impact of interannual rainfall variability on the spatial and temporal patterns of vegetation in a water-limited ecosystem. *Advances in Water Resources*, 27(1):83–95, 2004.

J. A. Foley, M. T. Coe, M. Scheffer, and G. Wang. Regime shifts in the sahara and sahel: interactions between ecological and climatic systems in northern africa. *Ecosystems*, 6(6):524–532, 2003.

K. T. Frank, B. Petrie, J. A. Fisher, and W. C. Leggett. Transient dynamics of an altered large marine ecosystem. *Nature*, 477(7362):86–89, 2011.

A. Gandhi, S. Levin, and S. Orszag. critical slowing down in time-to-extinction: an example of critical phenomena in ecology. *Journal of theoretical biology*, 192(3):363–376, 1998.

E. Gilad, J. Von Hardenberg, A. Provenzale, M. Shachak, and E. Meron. Ecosystem engineers: from pattern formation to habitat creation. *Physical Review Letters*, 93 (9):098105, 2004.

P. W. Glynn. El nifio warming, coral mortality and reef framework destruction by echinoid bioerosion in the eastern pacific. *Galaxea*, 7:129–160, 1988.

L. H. Gunderson. South florida: the reality of change and the prospects for sustainability: managing surprising ecosystems in southern florida. *Ecological economics*, 37(3):371–378, 2001.

V. Guttal and C. Jayaprakash. Changing skewness: an early warning signal of regime shifts in ecosystems. *Ecology Letters*, 11(5):450–460, 2008.

V. Guttal and C. Jayaprakash. Spatial variance and spatial skewness: leading indicators of regime shifts in spatial ecological systems. *Theoretical Ecology*, 2(1):3–12, 2009.

V. Guttal, C. Jayaprakash, and O. P. Tabbaa. Robustness of early warning signals of regime shifts in time-delayed ecological models. *Theoretical Ecology*, 6(3):271–283, 2013.

S. R. Hare and N. J. Mantua. Empirical evidence for north pacific regime shifts in 1977 and 1989. *Progress in oceanography*, 47(2):103–145, 2000.

H. Held and T. Kleinen. Detection of climate system bifurcations by degenerate fingerprinting. *Geophysical Research Letters*, 31(23), 2004.

R. HilleRisLambers, M. Rietkerk, F. van den Bosch, H. H. Prins, and H. de Kroon. Vegetation pattern formation in semi-arid grazing systems. *Ecology*, 82(1):50–61, 2001.

C. Holling. Engineering resilience versus ecological resilience. *Foundations of ecological resilience*, pages 51–66, 1996.

C. S. Holling. Resilience and stability of ecological systems. *Annual review of ecology and systematics*, pages 1–23, 1973.

T. P. Hughes. Catastrophes, phase shifts, and large-scale degradation of a caribbean coral reef. *Science-AAAS-Weekly Paper Edition*, 265(5178):1547–1551, 1994.

T. P. Hughes, C. Linares, V. Dakos, I. A. van de Leemput, and E. H. van Nes. Living dangerously on borrowed time during slow, unrecognized regime shifts. *Trends in ecology & evolution*, 28(3):149–155, 2013.

A. R. Ives. Measuring resilience in stochastic systems. *Ecological Monographs*, pages 217–233, 1995.

L. J. Jackson. Macrophyte-dominated and turbid states of shallow lakes: evidence from alberta lakes. *Ecosystems*, 6(3):213–223, 2003.

D. Karssenberg. Early-warning signals in ecogeomorphology: the example of a hillslope system. In *EGU General Assembly Conference Abstracts*, volume 13, page 12231, 2011.

D. Karssenberg. Slow or rapid collapse? transients between stable states as a source of uncertainty in predicting ecosystem shifts. In *Ames, D.P., Quinn, N.W.T., Rizzoli, A.E. (Eds.), Proceedings of the 7th International Congress on Environmental Modelling and Software, June 15-19, San Diego, California, USA.*, 2014.

D. Karssenberg and M. Bierkens. Catastrophic shifts in vegetation-soil systems may unfold rapidly or slowly independent of the rate of change in the system driver. 2014.

D. Karssenberg and M. F. Bierkens. Early-warning signals (potentially) reduce uncertainty in forecasted timing of critical shifts. *Ecosphere*, 3(2):art15, 2012.

D. Karssenberg, M. F. Bierkens, and M. Rietkerk. Catastrophic shifts in semi-arid vegetation-soil systems may unfold rapidly or slowly. *Manuscript in preparation*, 2015.

S. Kéfi. Reading the signs: Spatial vegetation patterns, arid ecosystems and desertification. *Gildeprint Drukkerijen BV, Enschede*, 2008.

S. Kéfi, M. Rietkerk, C. L. Alados, Y. Pueyo, V. P. Papanastasis, A. ElAich, and P. C. De Ruiter. Spatial vegetation patterns and imminent desertification in mediterranean arid ecosystems. *Nature*, 449(7159):213–217, 2007.

S. Kéfi, M. B. Eppinga, P. C. de Ruiter, and M. Rietkerk. Bistability and regular spatial patterns in arid ecosystems. *Theoretical Ecology*, 3(4):257–269, 2010.

S. Kéfi, V. Guttal, W. A. Brock, S. R. Carpenter, A. M. Ellison, V. N. Livina, D. A. Seekell, M. Scheffer, E. H. van Nes, and V. Dakos. Early warning signals of ecological transitions: Methods for spatial patterns. *PLoS ONE*, 9(3):e92097, 03 2014.

S. Kéfi, V. Guttal, W. A. Brock, S. R. Carpenter, A. M. Ellison, V. N. Livina, D. A. Seekell, M. Scheffer, E. H. van Nes, and V. Dakos. Early warning signals of ecological transitions: Methods for spatial patterns. *PloS one*, 9(3):e92097, 2014.

E. G. King, T. E. Franz, and K. K. Caylor. Ecohydrological interactions in a degraded two-phase mosaic dryland: implications for regime shifts, resilience, and restoration. *Ecohydrology*, 5(6):733–745, 2012.

T. Kleinen, H. Held, and G. Petschel-Held. The potential role of spectral properties in detecting thresholds in the earth system: application to the thermohaline circulation. *Ocean Dynamics*, 53(2):53–63, 2003.

N. Knowlton. Thresholds and multiple stable states in coral reef community dynamics. *American Zoologist*, 32(6):674–682, 1992.

J. A. Ludwig, D. J. Tongway, and S. G. Marsden. Stripes, strands or stipples: modelling the influence of three landscape banding patterns on resource capture and productivity in semi-arid woodlands, australia. *Catena*, 37(1):257–273, 1999.

J. A. Ludwig, B. P. Wilcox, D. D. Breshears, D. J. Tongway, and A. C. Imeson. Vegetation patches and runoff-erosion as interacting ecohydrological processes in semiarid landscapes. *Ecology*, 86(2):288–297, 2005.

R. H. MacArthur and E. O. Wilson. An equilibrium theory of insular zoogeography. *Evolution*, 17(4):373–387, 1963.

R. H. MacArthur and E. O. Wilson. *The theory of island biogeography*, volume 1. Princeton University Press, 1967.

R. M. May. Thresholds and breakpoints in ecosystems with a multiplicity of stable states. *Nature*, 269(5628):471–477, 1977.

Á. G. Mayor, S. Kéfi, S. Bautista, F. Rodríguez, F. Cartení, and M. Rietkerk. Feedbacks between vegetation pattern and resource loss dramatically decrease ecosystem resilience and restoration potential in a simple dryland model. *Landscape ecology*, 28 (5):931–942, 2013.

L. McCook. Macroalgae, nutrients and phase shifts on coral reefs: scientific issues and management consequences for the great barrier reef. *Coral reefs*, 18(4):357–367, 1999.

A. K. McDonald, R. J. Kinucan, and L. E. Loomis. Ecohydrological interactions within banded vegetation in the northeastern chihuahuan desert, usa. *Ecohydrology*, 2(1): 66–71, 2009.

MEA. *Ecosystems and human well-being: desertification synthesis*. World Resources Institute, Washington, DC, 2005.

E. Meron, E. Gilad, J. von Hardenberg, M. Shachak, and Y. Zarmi. Vegetation patterns along a rainfall gradient. *Chaos, Solitons & Fractals*, 19(2):367–376, 2004.

C. Montana. The colonization of bare areas in two-phase mosaics of an arid ecosystem. *Journal of Ecology*, 80(2):pp. 315–327, 1992.

G. T. Narisma, J. A. Foley, R. Licker, and N. Ramankutty. Abrupt changes in rainfall during the twentieth century. *Geophysical Research Letters*, 34(6), 2007.

I. Noy-Meir. Stability of grazing systems: an application of predator-prey graphs. *The Journal of Ecology*, pages 459–481, 1975.

M. Nyström, C. Folke, and F. Moberg. Coral reef disturbance and resilience in a human-dominated environment. *Trends in Ecology & Evolution*, 15(10):413–417, 2000.

B. Oborny, G. Meszéna, and G. Szabó. Dynamics of populations on the verge of extinction. *OIKOS*, 109(291Á/296), 2005.

J. D. Pelletier, S. B. DeLong, C. A. Orem, P. Becerra, K. Compton, K. Gressett, J. Lyons-Baral, L. A. McGuire, J. L. Molaro, and J. C. Spinler. How do vegetation bands form in dry lands? insights from numerical modeling and field studies in southern nevada, usa. *Journal of Geophysical Research: Earth Surface (2003–2012)*, 117(F4), 2012.

C. T. Perretti and S. B. Munch. Regime shift indicators fail under noise levels commonly observed in ecological systems. *Ecological Applications*, 22(6):1772–1779, 2012.

D. P. Peters, R. A. Pielke, B. T. Bestelmeyer, C. D. Allen, S. Munson-McGee, and K. M. Havstad. Cross-scale interactions, nonlinearities, and forecasting catastrophic events. *Proceedings of the National Academy of Sciences of the United States of America*, 101 (42):15130–15135, 2004.

P. S. Petraitis and S. R. Dudgeon. Experimental evidence for the origin of alternative communities on rocky intertidal shores. *Oikos*, 84(2):239–245, 1999.

J. Phelan, M. Norris, J. Warner, and M. Norris. *What Is Life?: A Guide to Biology*. W. H. Freeman, 2009. ISBN 9781429232166.

A. Porporato, F. Laio, L. Ridolfi, K. K. Caylor, and I. Rodriguez-Iturbe. Soil moisture and plant stress dynamics along the kalahari precipitation gradient. *Journal of Geophysical Research: Atmospheres (1984–2012)*, 108(D3), 2003.

J. R. Post, M. Sullivan, S. Cox, N. P. Lester, C. J. Walters, E. A. Parkinson, A. J. Paul, L. Jackson, and B. J. Shuter. Canada's recreational fisheries: the invisible collapse? *Fisheries*, 27(1):6–17, 2002.

J. F. Reynolds, D. M. S. Smith, E. F. Lambin, B. Turner, M. Mortimore, S. P. Batterbury, T. E. Downing, H. Dowlatabadi, R. J. Fernández, J. E. Herrick, et al. Global desertification: building a science for dryland development. *science*, 316(5826):847–851, 2007.

M. Rietkerk and J. Van de Koppel. Alternate stable states and threshold effects in semi-arid grazing systems. *Oikos*, pages 69–76, 1997.

M. Rietkerk, P. Ketner, J. Burger, B. Hoorens, and H. Olff. Multiscale soil and vegetation patchiness along a gradient of herbivore impact in a semi-arid grazing system in west africa. *Plant Ecology*, 148(2):207–224, 2000.

M. Rietkerk, M. C. Boerlijst, F. van Langevelde, R. HilleRisLambers, J. van de Koppel, L. Kumar, H. H. Prins, and A. M. de Roos. Self-organization of vegetation in arid ecosystems. *The American Naturalist*, 160(4):524–530, 2002.

M. Rietkerk, S. C. Dekker, P. C. de Ruiter, and J. van de Koppel. Self-organized patchiness and catastrophic shifts in ecosystems. *Science*, 305(5692):1926–1929, 2004.

P. Saco and J. Rodriguez. 2.14 modeling ecogeomorphic systems. In J. F. Shroder, editor, *Treatise on Geomorphology*, pages 201 – 220. Academic Press, San Diego, 2013.

P. Saco, G. Willgoose, and G. Hancock. Eco-geomorphology of banded vegetation patterns in arid and semi-arid regions. *Hydrology & Earth System Sciences*, 11(6), 2007.

P. M. Saco and M. Moreno-de las Heras. Ecogeomorphic coevolution of semiarid hillslopes: Emergence of banded and striped vegetation patterns through interaction of biotic and abiotic processes. *Water Resources Research*, 49(1):115–126, 2013.

M. Scheffer. *Ecology of shallow lakes*. Springer, 2004.

M. Scheffer. *Critical transitions in nature and society*. Princeton University Press, 2009.

M. Scheffer and S. R. Carpenter. Catastrophic regime shifts in ecosystems: linking theory to observation. *Trends in ecology & evolution*, 18(12):648–656, 2003.

M. Scheffer and E. Jeppesen. Regime shifts in shallow lakes. *Ecosystems*, 10(1):1–3, 2007.

M. Scheffer, S. Hosper, M. Meijer, B. Moss, and E. Jeppesen. Alternative equilibria in shallow lakes. *Trends in ecology & evolution*, 8(8):275–279, 1993.

M. Scheffer, S. Rinaldi, A. Gragnani, L. R. Mur, and E. H. van Nes. On the dominance of filamentous cyanobacteria in shallow, turbid lakes. *Ecology*, 78(1):272–282, 1997.

M. Scheffer, S. Carpenter, J. A. Foley, C. Folke, and B. Walker. Catastrophic shifts in ecosystems. *Nature*, 413(6856):591–596, 2001.

M. Scheffer, S. Szabó, A. Gragnani, E. H. Van Nes, S. Rinaldi, N. Kautsky, J. Norberg, R. M. Roijackers, and R. J. Franken. Floating plant dominance as a stable state. *Proceedings of the national academy of sciences*, 100(7):4040–4045, 2003.

M. Scheffer, J. Bascompte, W. A. Brock, V. Brovkin, S. R. Carpenter, V. Dakos, H. Held, E. H. Van Nes, M. Rietkerk, and G. Sugihara. Early-warning signals for critical transitions. *Nature*, 461(7260):53–59, 2009.

M. Scheffer, S. R. Carpenter, T. M. Lenton, J. Bascompte, W. Brock, V. Dakos, J. Van De Koppel, I. A. Van De Leemput, S. A. Levin, E. H. Van Nes, et al. Anticipating critical transitions. *science*, 338(6105):344–348, 2012.

W. H. Schlesinger, J. F. Reynolds, G. L. Cunningham, L. F. Huenneke, W. M. Jarrell, R. A. Virginia, and W. G. Whitford. Biological feedbacks in global desertification. *Science(Washington)*, 247(4946):1043–1048, 1990.

O. J. Schmitz, E. L. Kalies, and M. G. Booth. Alternative dynamic regimes and trophic control of plant succession. *Ecosystems*, 9(4):659–672, 2006.

D. A. Seekell, S. R. Carpenter, and M. L. Pace. Conditional heteroscedasticity as a leading indicator of ecological regime shifts. *The American Naturalist*, 178(4):442–451, 2011.

J. A. Sherratt. Pattern solutions of the klausmeier model for banded vegetation in semiarid environments v: The transition from patterns to desert. *SIAM Journal on Applied Mathematics*, 73(4):1347–1367, 2013.

J. H. Steele. Regime shifts in fisheries management. *Fisheries Research*, 25(1):19–23, 1996.

R. S. Steneck, M. H. Graham, B. J. Bourque, D. Corbett, J. M. Erlandson, J. A. Estes, and M. J. Tegner. Kelp forest ecosystems: biodiversity, stability, resilience and future. *Environmental conservation*, 29(04):436–459, 2002.

S. H. Strogatz. Nonlinear dynamics and chaos: W ith applications to physics, biology, chemistry, and engineering. *Studies in Nonlinearity. Reading, MA: Addison-WesleyPublishing Co*, 1994.

J. Thiery, J.-M. d'Herbes, and C. Valentin. A model simulating the genesis of banded vegetation patterns in niger. *Journal of Ecology*, pages 497–507, 1995.

R. Thom. Stabilité structurelle et morphogénèse. *Poetics*, 3(2):7–19, 1974.

D. J. Tongway and J. A. Ludwig. Theories on the origins, maintenance, dynamics, and functioning of banded landscapes. In *Banded vegetation patterning in arid and semiarid environments*, pages 20–31. Springer, 2001.

C. Valentin, J.-M. d'Herbès, and J. Poesen. Soil and water components of banded vegetation patterns. *Catena*, 37(1):1–24, 1999.

E. H. Van Nes and M. Scheffer. Slow recovery from perturbations as a generic indicator of a nearby catastrophic shift. *The American Naturalist*, 169(6):738–747, 2007.

J. von Hardenberg, E. Meron, M. Shachak, and Y. Zarmi. Diversity of vegetation patterns and desertification. *Physical Review Letters*, 87(19):198101, 2001.

J. von Hardenberg, A. Y. Kletter, H. Yizhaq, J. Nathan, and E. Meron. Periodic versus scale-free patterns in dryland vegetation. *Proceedings of the Royal Society B: Biological Sciences*, 277(1688):1771–1776, 2010.

B. H. Walker. Rangeland ecology: Understanding and managing change. *Ambio*, 22: 80–86, 1993.

C. Walters and J. F. Kitchell. Cultivation/depensation effects on juvenile survival and recruitment: implications for the theory of fishing. *Canadian Journal of Fisheries and Aquatic Sciences*, 58(1):39–50, 2001.

R. Wang, J. A. Dearing, P. G. Langdon, E. Zhang, X. Yang, V. Dakos, and M. Scheffer. Flickering gives early warning signals of a critical transition to a eutrophic lake state. *Nature*, 492(7429):419–422, 2012.

H. Wheater, S. Sorooshian, K. D. Sharma, et al. *Hydrological modelling in arid and semi-arid areas.* Cambridge University Press, 2008.

L. White. Vegetation arcs in jordan. *The Journal of Ecology*, pages 461–464, 1969.

B. P. Wilcox, D. D. Breshears, and C. D. Allen. Ecohydrology of a resource-conserving semiarid woodland: effects of scale and disturbance. *Ecological Monographs*, 73(2): 223–239, 2003.

G. Willgoose, R. L. Bras, and I. Rodriguez-Iturbe. A coupled channel network growth and hillslope evolution model: 1. theory. *Water Resources Research*, 27(7):1671–1684, 1991.

C. Wissel. A universal law of the characteristic return time near thresholds. *Oecologia*, 65(1):101–107, 1984.

B. Worm, H. Lotze, C. Boström, R. Engkvist, V. Labanauskas, and U. Sommer. Marine diversity shift linked to interactions among grazers, nutrients and propagule banks. *Marine Ecology Progress Series*, 185:309–314, 1999.